Report No: P WMA
19/G10/00/2413/3

Department of Water Affairs
Directorate: Options Analysis

PRE-FEASIBILITY AND FEASIBILITY STUDIES FOR AUGMENTATION OF THE WESTERN CAPE WATER SUPPLY SYSTEM BY MEANS OF FURTHER SURFACE WATER DEVELOPMENTS

REPORT No.1 – VOLUME 3
Berg Estuary Environmental Water Requirements

APPENDIX No.C

Specialist Report - Physical Dynamics and Water Quality

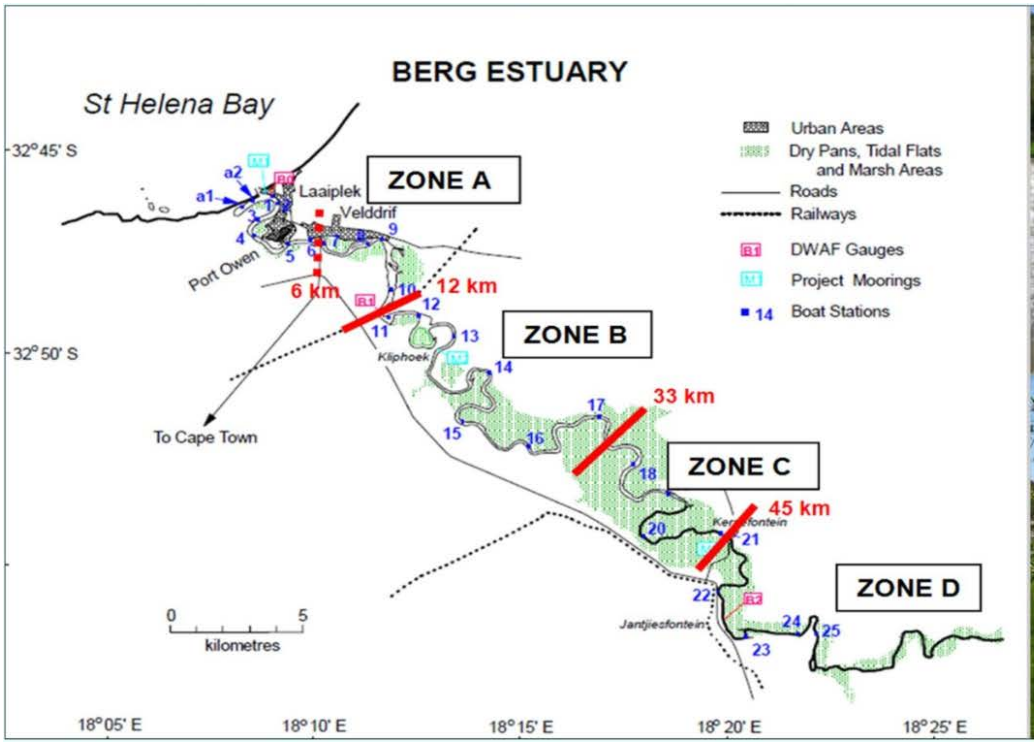

June 2012

STUDY REPORT LIST

REPORT No	REPORT TITLE	VOLUME No.	DWA REPORT No.	VOLUME TITLE
1	ECOLOGICAL WATER REQUIREMENT ASSESSMENTS	Vol 1	PWMA19 G10/00/2413/1	**Riverine Environmental Water Requirements**
				Appendix 1: EWR data for the Breede River
				Appendix 2: EWR data for the Palmiet River
				Appendix 3: EWR data for the Berg River
				Appendix 4: Task 3.1: Rapid Reserve assessments (quantity) for the Steenbras, Pombers and Kromme Rivers
				Appendix 5: Habitat Integrity Report – Breede River
		Vol 2	PWMA19 G10/00/2413/2	**Rapid Determination of the Environmental Water Requirements of the Palmiet River Estuary**
				Appendix A: Summary of data available for the RDM investigations undertaken during 2007 and 2008
				Appendix B: Summary of baseline data requirements and the long-term monitoring programme
				Appendix C: Abiotic Specialist Report
		Vol 3	PWMA19 G10/00/2413/3	**Berg Estuary Environmental Water Requirements**
				Appendix A: Available information and data
				Appendix B: Measurement of streamflows in the Lower Berg downstream of Misverstand Dam
				Appendix C: Specialist Report – Physical dynamics and water quality
				Appendix D: Specialist Report – Modelling
				Appendix E: Specialist Report – Microalgae
				Appendix F: Specialist Report – Invertebrates
				Appendix G: Specialist Report – Fish
				Appendix H: Specialist Report – Birds
				Appendix I: Specialist Report – The economic value of the Berg River Estuary
2	PRELIMINARY ASSESSMENT OF OPTIONS		PWMA19 G10/00/2413/4	Appendix 1: Scheme Yield Assessments and Diversion Functions
				Appendix 2: Unit Reference Value Calculation Sheets
				Appendix 3: Yield Analysis and Dam Size Optimization
				Appendix 4: Dam Design Inputs
				Appendix 5: Diversion Weir Layout Drawings
				Appendix 6: Voëlvlei Dam Water Quality Assessment
				Appendix 7: Botanical Considerations
				Appendix 8: Heritage Considerations
				Appendix 9: Agricultural Economic Considerations

STUDY REPORT LIST (cntd)

REPORT No	REPORT TITLE	VOLUME No.	DWA REPORT No.	VOLUME TITLE
3	FEASIBILITY STUDIES	Vol 1	PWMA19 G10/00/2413/5	**Berg River-Voëlvlei Augmentation Scheme**
				Appendix 1: Updating of the Western Cape Water Supply System Analysis for the Berg River-Voëlvlei Augmentation Scheme
				Appendix 2: Configuration, Calibration and Application of the CE-QUAL-W2 model to Voëlvlei Dam for the Berg River-Voëlvlei Augmentation Scheme
				Appendix 3: Monitoring Water Quality During Flood Events in the Middle Berg River (Winter 2011), for the Berg River-Voëlvlei Augmentation Scheme
				Appendix 4: Dispersion Modelling in Voëlvlei Dam from Berg River Water Transfers for the Berg River-Voëlvlei Augmentation Scheme
				Appendix 7 - 12: See list under Volume 2 below
		Vol 2	PWMA19 G10/00/2413/6	**Breede-Berg (Michell's Pass) Water Transfer Scheme**
				Appendix 5: Scheme Operation and Yield Analyses with Ecological Flow Requirements for the Breede-Berg (Michell's Pass) Water Transfer Scheme
				Appendix 6: Preliminary Design of Papenkuils Pump Station Upgrade and Pre-Feasibility Design of the Boontjies Dam, for the Breede-Berg (Michell's Pass) Water Transfer Scheme
				Appendix 7: Ecological Water Requirements Assessment Summary for the Berg River-Voëlvlei Augmentation Scheme , and the Breede Berg (Michell's Pass) Water Transfer Scheme
				Appendix 8: Geotechnical Investigations for the Berg River-Voëlvlei Augmentation Scheme, and the Breede-Berg (Michell's Pass) Water Transfer Scheme
				Appendix 9: LiDAR Aerial Survey, for the Berg River-Voëlvlei Augmentation Scheme, and the Breede-Berg (Michell's Pass) Water Transfer Scheme
				Appendix 10: Conveyance Infrastructure Design Report, for the Berg River-Voëlvlei Augmentation Scheme, and the Breede-Berg (Michell's Pass) Water Transfer Scheme
				Appendix 11: Diversion Weirs Design for the Berg River-Voëlvlei Augmentation Scheme, and the Breede-Berg (Michell's Pass) Water Transfer Scheme
				Appendix 12: Cost Estimates for the Berg River-Voëlvlei Augmentation Scheme, and the Breede-Berg (Michell's Pass) Water Transfer Scheme
4	RECORD OF IMPLEMENTATION DECISIONS		PWMA19 G10/00/2413/7	

STUDY REPORT MATRIX DIAGRAM

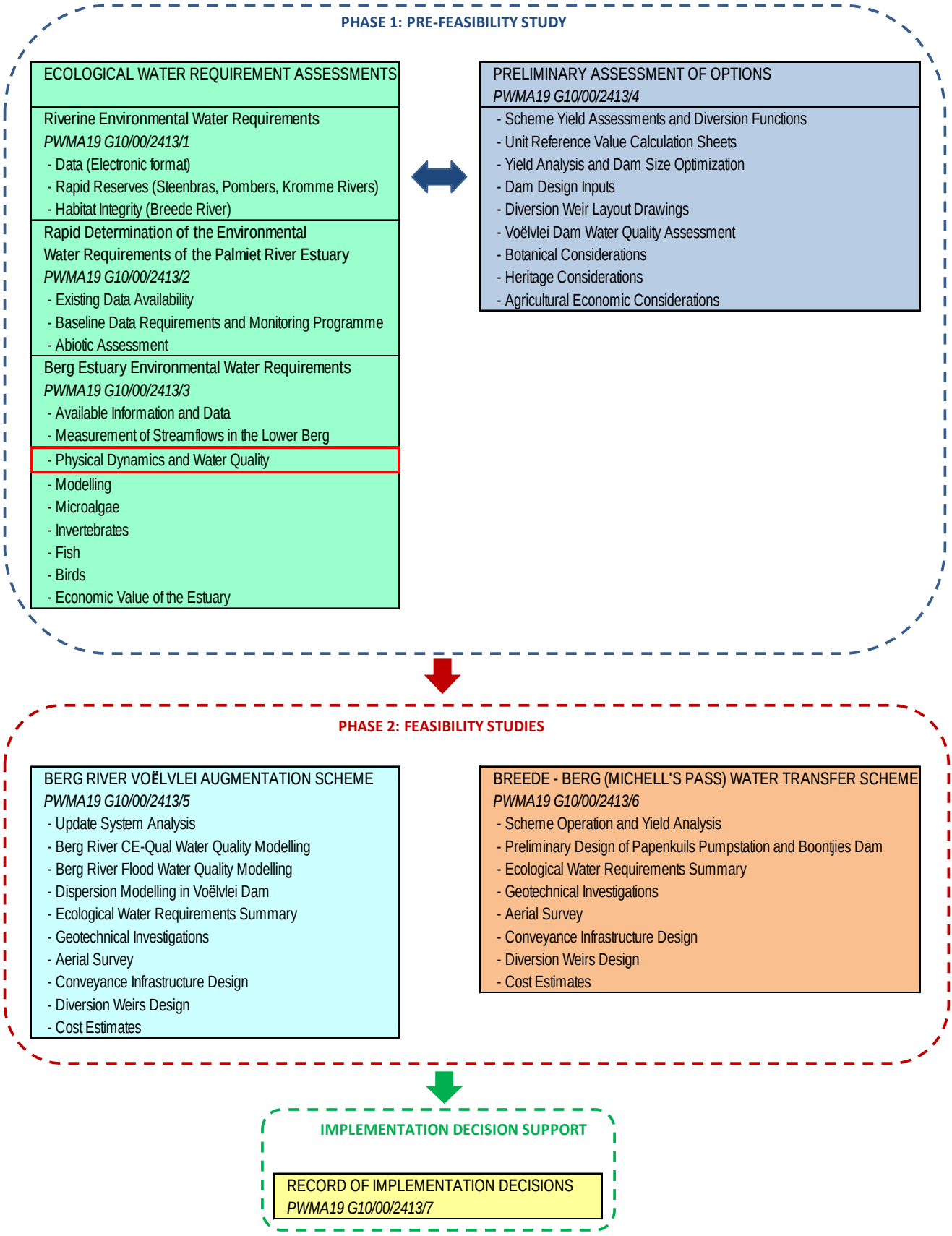

ACKNOWLEDGEMENTS

PREPARED FOR THE WCWC JV BY:
CSIR, Environmentek
P O Box 320
7599
STELLENBOSCH

AUTHORS:
S. Taljaard, L. van Niekerk, R. van Ballegooyen, A. Theron, P. Huizinga

REVIEWER:
C.A. Brown

LEAD CONSULTANT:
Anchor Environmental

EDITOR:
B. Clark

TABLE OF CONTENTS

LIST OF FIGURES

LIST OF TABLES

1 Brief

The CSIR was contracted by Anchor Environmental Consultants to provide specialist input on the physical dynamics and water quality for the determination of estuarine ecological water requirements on the Great Berg Estuary.

The Ecological Water requirement studies on the estuaries will follow the methods as described in Resource Directed Measures for Protection of Water Resources: Methodologies for the determination of ecological water requirements for estuaries Version 2 (DWAF, 2008).

The assessment was based on available data that was collected during an intense monitoring programme during 2002 to 2005 (DWAF, 2007). A 3-dimensional hydrodynamic modelling (DELFT 3D FLOW) study was also undertaken on the Great Berg Estuary to refine understanding of the influence of river flows on hydrodynamic and sediment processes.

This report contains the results from the abiotic specialist study (physical dynamics and water quality).

2 Assumption and Limitations

The brief was undertaken based on the following assumptions:

- No new data were collected as part of this study. It was based on the information collated and collected during the intensive monitoring programme conducted on the Great Berg system in 2002-2005 (DWAF, 2007);
- It is assumed that the simulated run-off scenarios (50 – 70 years), representative of river inflow at the head of the Great Berg Estuary provided to the CSIR are correct. These scenarios included the reference condition, the present state and a range of additional scenarios as agreed between the CSIR, Anchor Environmental Consultants and DWAF;
- Numerical modelling was based on available information, *e.g.* bathymetry and sediment data provided by Anchor Environmental Consulting. No new data will be collected as part of this study;
- Hydrodynamic modelling only comprised of the water column and inundation of the floodplain under various scenarios provided by Anchor Environmental Consultants (through DWAF); and
- No sediment modelling was undertaken as part of this study.

3 Study Area

The Berg River catchment has a total area of 6420 km^2 (Figure 3.1). Of this, 4010 km^2 is located upstream of the lowest hydrological monitoring point at Die Brug gauging station (G1M31) which is situated downstream of Misverstand Dam. The river flows through mountainous terrain from its source at an altitude of 1522 m in the Groot Drakenstein Mountains, to the town of Paarl. Whereas the eastern catchment boundary remains mountainous as far north as Porterville, the river itself flows through undulating agricultural lands from Paarl to the sea. The Great Berg River Estuary enters the sea at St Helena Bay on the Cape west coast. The estuary mouth lies at 32^{o}46'S; 18^{o}08'E.

The Berg River region has a Mediterranean climate and falls within the winter rainfall region of the Western Cape. The rainfall is mainly of a cyclonic nature originating over the Atlantic Ocean. Frontal systems encountering the mountain ranges of the Upper Berg catchment rise causing orographic rainfall. As a result of both its close proximity to Cape Town, and its highly reliable run-off characteristics, the water resources of the Berg River have been developed increasingly during the last 60 years.

The Berg River Estuary (Figure 3.1) is long and sinuous as a result of the riverbed falling only one metre in the last 50 km (Day, 1981).

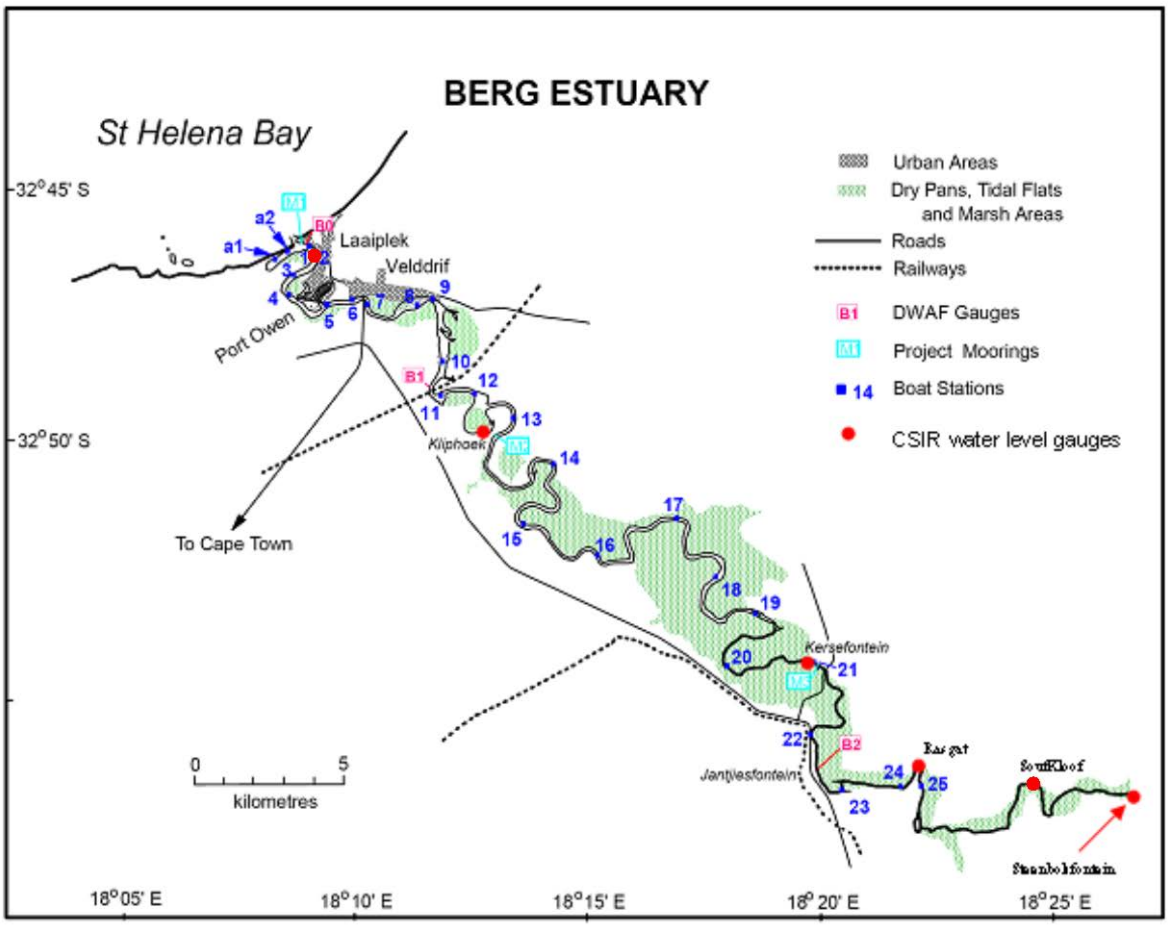

Figure 3.1 Map of the Great Berg River Estuary (adapted from Schumann, 2007)

The head of an estuary is typically defined as the extent of tidal influence, which is not necessarily the extent of saline intrusion. In the case of the Great Berg estuary, tidal influence extends ~70 km upstream of the mouth. This together, with the extensive salt marshes on the floodplain, which might be regarded as part of the estuarine area, makes it difficult to calculate the total area of the Berg River estuary. A portion of the estuarine area from the mouth up to the Sishen-Saldanha railway bridge was given as 798 ha by Duvenhage (1983). This area comprises of 144 ha intertidal mudflats, 242 ha of saltmarsh, 222 ha of commercial saltworks and 190 ha of open water.

The original mouth lay approximately one kilometre south of the present artificial mouth. Gradual sedimentation of the natural estuary mouth rendered navigation hazardous. Means of improving access via the natural estuary mouth were investigated, but rock, lying at shallow depths for at least 600 m seawards of the mouth, rendered this option uneconomic. It was then decided to construct an artificial mouth one kilometre north of the natural mouth. This mouth, opened in December 1966, has fulfilled its intended purpose of improving access for fishing vessels to Laaiplek and Velddrif independently of the state of the tide. The remains of the former mouth channel now form the so-called 'blind arm'.

4 Available Data

The following data were available for this study:

DATA REQUIRED	AVAILABILITY	REFERENCE
Simulated monthly runoff data (at the head of the estuary) for present state, reference condition and the selected runoff scenarios over 50 to 70 years	77 year period	Aurecon
Simulated flood hydrographs for present state, reference condition and runoff scenarios: 1:1, 1:2, 1:5 floods (influencing aspects such as floodplain inundation) 1:20, 1:50, 1:100, 1:200 year floods (long-term sediment dynamics, equilibrium, budget)	None	Inferred from DWAF 2007
Aerial photographs of estuary (earliest available year as well as most recent)	Available	
Continuous water level recordings near mouth of estuary	Laaiplek G1H074 - 1980 Kliphoek G1H024 - 1980 Jantjiesfontein G1H023 - 2003	DWAF
Mouth observations		
Longitudinal salinity and temperature profiles (in situ) collected over a spring and neap tide during high and low tide at: end of low flow season peak of high flow season	Oct 1975; Aug 1976; Sep1989; Jan/Feb 1990; Aug 1995, Feb 1996; Mar 1996; Nov 2002 – Nov 2005 (13 sampling surveys)	Eagle and Bartlett, 1984; Taljaard et al, 1992; Slinger and Taljaard, 1996; Slinger et al, 1996; Schumann, 2007
Water quality measurements (*i.e.* system variables, and nutrients) taken along the length of the estuary (surface and bottom samples) on a spring and neap high tide at: end of low flow season and peak of high flow season	Oct 1975; Aug 1976; Sep1989; Jan/Feb 1990; Aug 1995, Feb 1996; Mar 1996; Feb, May, Aug, Nov 2005	Eagle and Bartlett, 1984; Taljaard et al, 1992; Slinger and Taljaard, 1996; Slinger et al, 1996; Clark and Taljaard, 2007)
Measurements of organic content and toxic substances (*e.g*. trace metals and hydrocarbons) in sediments along length of the estuary.		
Water quality (*e.g*. system variables, nutrients and toxic substances) measurements on river water entering at the head of the estuary	1976 to 2007 (Jantjiesfontein); 1976-2008 (Die Brug, Misverstand)	Jantjiesfontein - G1H023Q01 Misverstand, Die Brug - G1H031Q01
Water quality (*e.g*. system variables, nutrients and toxic substances) measurements on near-shore seawater	Available data	DWAF, 1995; Schumann, 2007

5 Typical Abiotic States

Based on the data and information on the Great Berg Estuary, five typical abiotic states were identified for this system, related to tidal exchange, salinity distribution and water quality. These are primarily determined by river inflow patterns, state of the tide and wave conditions. The different states are listed in Table 5.1. In characterising the hydrodynamic and water quality characteristics within each abiotic state the estuary was sub-divided into 4 distinct zone, as illustrated in Figure 5.1. The zones were derived largely from typical salinity distributions and channel bathymetry.

Table 5.1 Typical abiotic states of the Great Berg Estuary

STATE	BRIEF DESCRIPTION	MONTHLY FLOW RANGE (m^3/s)
1	Severe marine-dominated - saline intrusion extends further than 45 km upstream of mouth (*i.e*. into Zone D, see Figure 5.1)	<0.5
2	Marine-dominated - saline intrusion extends up to 45 km from mouth (i.e. downstream of Zone D, see Figure 5.1)	0.5 - 1
3	Small to medium freshwater inflow – marine influence evident up to 33 km from mouth (i.e. downstream of Zone C), with strong freshwater influence in upper ~40 km (*i.e*. in Zones C and D)	1 - 5
4	Medium to high freshwater inflow – marine influence only evident up to 12 km from mouth (*i.e*. downstream of Zone B), with strong freshwater influence in upper ~60 km (i.e. in Zones B-D)	5 - 25
5	Freshwater-dominated – estuary is fresh throughout (*i.e.* Zones A-D), except during spring tides when seawater intrusion may extend up to 6 km from mouth into Zone A during high tides	>25

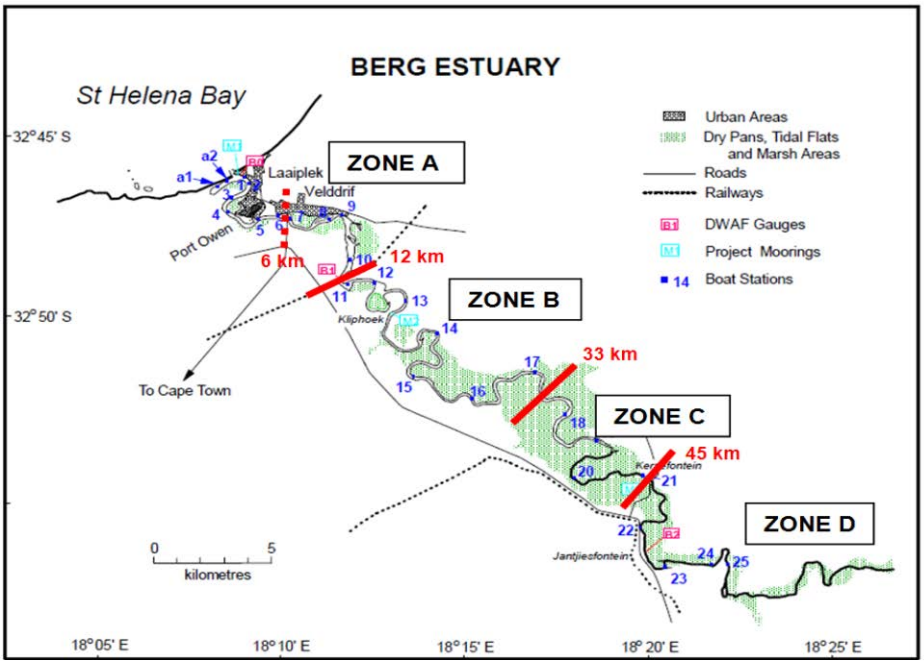

Figure 5.1 Different abiotic zones identified for the Great Berg Estuary (map adapted from Schumann, 2007)

The physical and water quality characteristics associated with each of the above abiotic states is discussed in greater detail in the following chapters.

6 Hydrodynamics

The hydrodynamics of the Berg River estuary are complex, owing to the extreme variation in inflow conditions from winter to summer, the gentle gradient (1 meter in the last 50 km; Day, 1981) and the length of the estuary.

6.1 Water levels

6.1.1 Tidal variability

Tidal oscillation of water levels was recorded 69 kilometres upstream in the estuary. Tides along the South African coast fall into the semi-diurnal microtidal category, with spring tide amplitudes seldom reaching above 2 m, and with neap tide amplitudes as small as 0.5 m. Shillington (1984) has described the existence of edge waves with periods of 20 to 60 minutes, which reached an amplitude of 1.5 m near the Orange River some 500 km to the north. Subtidal coastal trapped waves with typical amplitudes around 30 cm have been described by de Cuevas *et al*. (1986), while Brundrit (1984) investigated variability on monthly and seasonal scales. Furthermore, Hughes *et al*. (1991) demonstrated that there was a sea level rise of about 1.2 mm/yr, consistent with other tectonically stable world trends.

During March 1990 six water level recorders were installed by the CSIR in the Berg River estuary for a few weeks. To illustrate the complexity of tidal variation, data collected on 12 March 1990 are used (Figure 6.1). The recorded water level variation immediately inside the mouth was the same as the predicted tidal variation at Saldanha Bay, which implies that the present mouth does not reduce tidal variation. Between the mouth and the farm Kliphoek, 14 km upstream, a reduction in tidal amplitude of about 67% occurs. A slight amplification in tidal variation takes place between

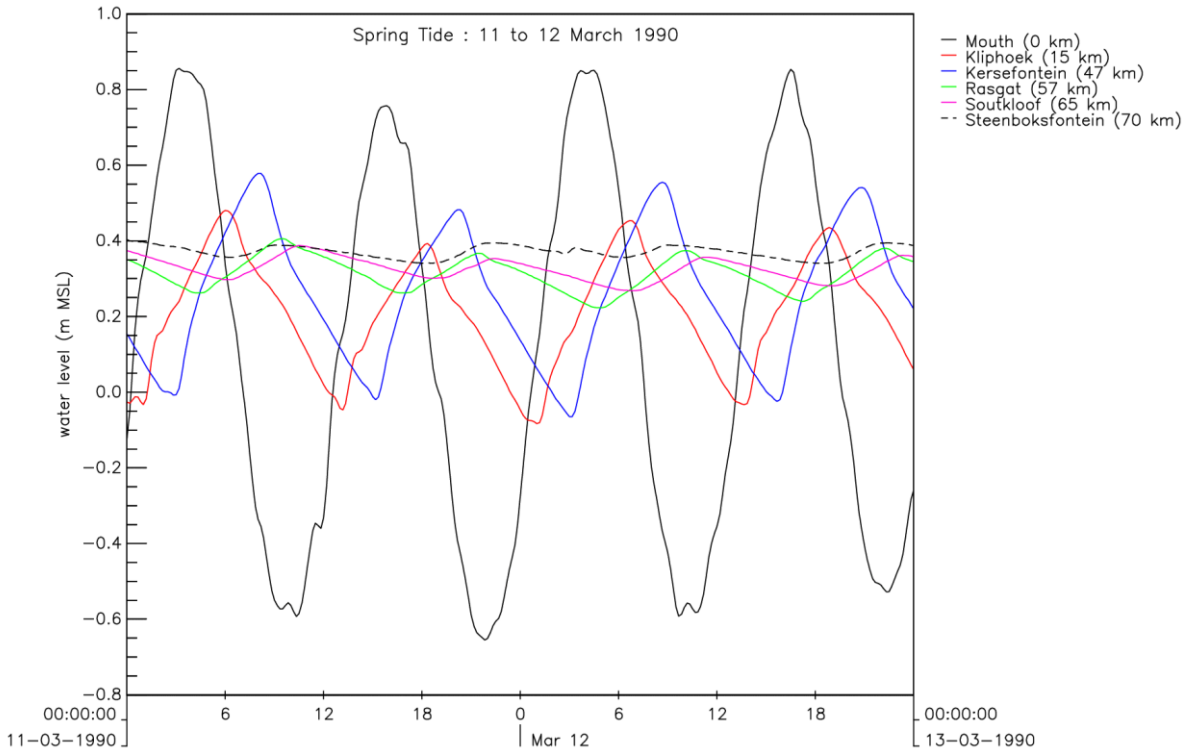

Figure 6.1 Water level variations measured at six positions in the Berg Estuary on 11 and 12 March 1990

Kliphoek and Kersefontein, 46 km upstream of the mouth. Such amplifications in tidal variation are known to occur in estuaries and are usually caused by funnelling as the estuary becomes shallower and narrower with distance upstream.

At Rasgat (55 km upstream), Soutkloof (63 km upstream) and Steekboksfontein (68.5 km upstream) further reduction take place, but the tidal variation is still noticeable.

The water depth varies considerably along the length of the estuary and there are quite wide tidal flats with very shallow areas. Water depth in the estuary varies with the tide, affecting the speed of the tidal wave, however the lags in tidal variations along the estuary are predominantly a frictional effect. Slinger and Taljaard (1994) reported that high tide lagged the mouth by 4 hours at Kliphoek and by 2.3 hours at low tide. At a position 56 km from the mouth the lags were 7 hours and 6.7 hours at low and high tides; note that they did not consider the effects of the longer-period water level variations. A more detailed analysis of tidal lags from both the CSIR March 1990 water levels recordings and measured water levels from DWAF water level recorders is given in Table 6.1 below.

Due to these tidal delays the flow direction in the upper estuary can be opposite to those at the mouth (Huizinga *et al*., 1994; Slinger and Taljaard, 1994).

Table 6.1 Tidal range and normalised tidal range (normalised by tidal range at the mouth of the estuary) at various locations on the Berg River Estuary

Site	Distance upstream (m)	Spring tide		Neap tide	
		Tidal lag (trough)	Tidal lag (peak)	Tidal lag (trough)	Tidal lag (peak)
Mouth (CSIR 1990)	0	0 m	0 m	0.60	1.00
Laaiplek (G1H074)	545	35 m*	35 m*	-	-
Kliphoek (G1H024)	11300	3h 24m*	3h 07m*	-	-
Kliphoek (CSIR 1990)	15000	3h 14m	2h 42m	2h 50m	2h 50m
Kersefontein (CSIR 1990)	46990	5h 16m	4h 42m	4h 37	3h 35m
Jantjiesfontein (G1H023)	51000	6h 40 m*	6h 22m*	-	-
Rasgat (CSIR 1990)	57528	6h 57m	6h 05m	6h 24m	5h 27m
SoutKloof (CSIR 1990)	65070	7h 00m	7h 12m	6h 55m	6h 43m
Steenbokfontein (CSIR 1990)	70987	8h 50m	8h 28m	-	-

** tidal lags (compared to Saldanha Bay water level measurements) as reported by Schumann and Brink (2009) for a period between spring and neap tides.*

Continuous water level data is also available from three permanently installed water level gauges in the estuary (See Table 6.2).

Table 6.2 Continuous water level recorders in the Berg Estuary

Site	DWAF gauge ID	Start
Kliphoek	G1H024	1980.10.01
Jantjiesfontein	G1H023	1980.10.01
Laaiplek	G1H074	2003.10.21

Figure 6.2 depicts the tidal variability at the Saldanha Bay and the three permanently water level gauges. With the long-period fluctuations removed, the regularity of the tides is evident within the envelope of the spring-neap variability. The diurnal inequality is appreciable at times, though it is not consistent. Table 3.10 gives a maximum tidal variation at Saldanha Bay of 1.74m, reducing to 1.60m at Laaiplek, 0.61m at Kliphoek and finally 0.24m at Jantjiesfontein (DWAF 2007).

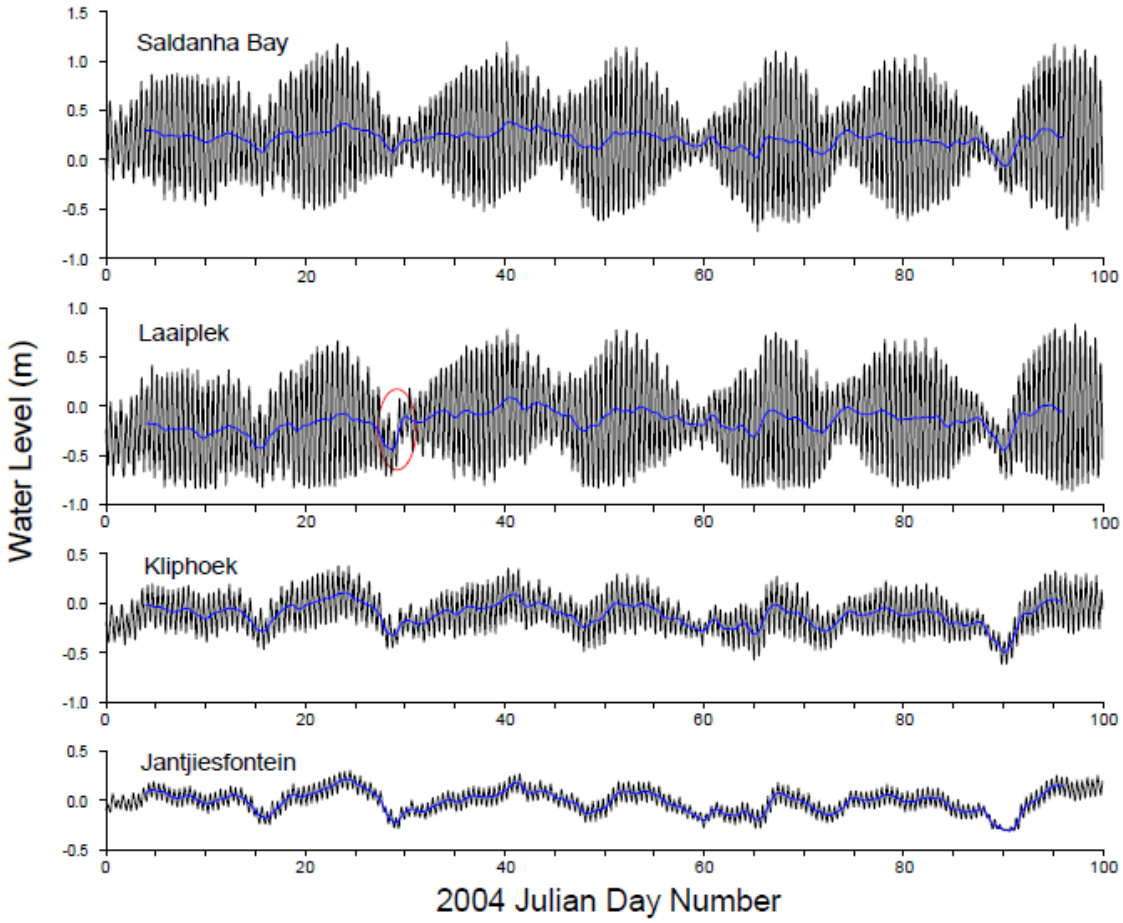

Figure 6.2 Measured water level relative to msl at Saldanha Bay, Laaiplek, Kliphoek and Jantjiesfontein. The blue lines show the longer-period fluctuations, while the situation at the red ellipse is discussed in the text (Source: DWAF 2007)

Figure 6.2 shows the actual measured time series of water level at the four sites, together with the superimposed longer-period variability (in blue). The semidiurnal tidal variability is the dominant component at Saldanha Bay and Laaplek, while it is apparent that the diurnal tide contributes to a diurnal inequality. In addition the two-week spring-neap cycle is clearly evident (DWAF 2007). The longer-period fluctuations serve to alter the extent of the tidal oscillations by changing the background water level, though it is important to realise that the periodicity is not affected.

Nonetheless, it is not altogether uncommon in estuaries that, for instance, a high tide on one day can be lower than a low tide on the next day. This effect is evident on day 30 in the Laaiplek series, where the midnight high tide on day 29 was only marginally higher than the afternoon low tide the next day, while the following low tide was actually higher (shown by the red circle on the figure). Higher up in the estuary at Jantjiesfontein this is a regular occurrence. The tidal components are reduced considerably at Kliphoek[1], and even more so at Jantjiesfontein. At the same time it is apparent that the longer-period fluctuations are amplified and at Jantjiesfontein it is these effects that have the largest influence on water level.

Maximum tidal variation at Saldanha Bay is 1.74 m, reducing to 1.60 m at Laaiplek, 0.61 m at Kliphoek and finally 0.24 m at Jantjiesfontein (see Table 6.3) (DWAF 2007).

Table 6.3 Minimum and maximum water levels, and overall variation measured at Saldanha Bay, Laaiplek, Kliphoek and Jantjiesfontein from November to November 2005 (DWAF 2007)

Site	Min (m)	Max (m)	Var (m)	Site	Min (m)	Max (m)	Var (m)
Saldanha Bay	0.86	1.38	2.24	Kliphoek	0.64	0.66	1.30
Laaiplek	-0.86	1.07	1.93	Jantjiesfontein	-0.32	2.69	3.01

The water depth varies considerably along the length of the estuary and there are quite wide tidal flats with very shallow areas. It is also important to note that the depth varies with the tide, thus also affecting the speed of the tidal wave.

Nonetheless, the estimated wave depths are small, probably also a consequence of frictional effects, which are not incorporated into the shallow-wave equation. Slinger and Taljaard (1994) found that high tide lagged the mouth by 4 hours at Kliphoek and by 2.3 hours at low tide. At a position 56 km from the mouth the lags were 7 hours and 6.7 hours at low and high tides, in approximate agreement with values found here; note that they did not consider the effects of the longer-period variations.

Table 6.4 lists the propagation speeds of the tidal signal in the Berg Estuary. The calculated water depth from the shallow water wave speed is also given. Note that constrictions in the mouth area mean that additional factors affect the lag at Laaiplek, and this is taken as the starting point for the tidal signal (DWAF 2007).

[1] The DWAF gauge indentified as the Kliphoek water level gauge is actually located downstream of they Railway Bridge (see DWAF water level gauge B1 in Figure 3.21) and should in Reality be called the “Railway Bridge” water level gauge as this would be less misleading in terms of its location.

Table 6.4 Time lags and propagation speeds of the tidal signal in the Berg Estuary

Site	Distance (km)	Tidal Peak Lag	Tidal Trough Lag	Speed (m/s)	Depth (m)
Saldanha Bay	0.0	00:00	00:00		
Laaiplek	0.4	35 m	35 m		
Kliphoek	16.8	3 h 7 m	3 h 24 m	1.77	0.32
Jantjiesfontein	53.5	6 h 22 m	6 h 40 m	2.50	0.64

6.1.2 Longer-period variability

Subtidal water level fluctuations are observed along the entire length of the estuary. These subtidal water level fluctuations have typical amplitudes of 15 to 20 cm, ranging up to 30 cm or more on occasion. Negative fluctuations in subtidal water levels are associated with S to SE wind conditions offshore and associated upwelling of cold waters, while positive fluctuations are associated with NW offshore winds and downwelling.

Figure 6.3 shows the water level variability at periods longer than the diurnal tidal period (DWAF 2007). Note the amplification of the signal immediately within the estuary at Laaiplek, and then the further undiminished propagation up to Jantjiesfontein. The longer-period oceanic water level variations are more noticeable in the upper reaches of the Berg Estuary than tidal variations.

Vertical lines have been drawn at significant peaks and troughs on Figure 6.3 in order to estimate propagation speeds of these longer-period oceanic signals. It is apparent that Laaiplek leads Saldanha Bay, and this is consistent with the existence of coastal trapped waves which travel southwards along the west coast, and therefore reach St Helena Bay before Saldanha Bay. These longer-period waves travel as shallow-water waves up the estuary, and rough estimates for a lag between Laaiplek and Jantjiesfontein give values around 10 hours.

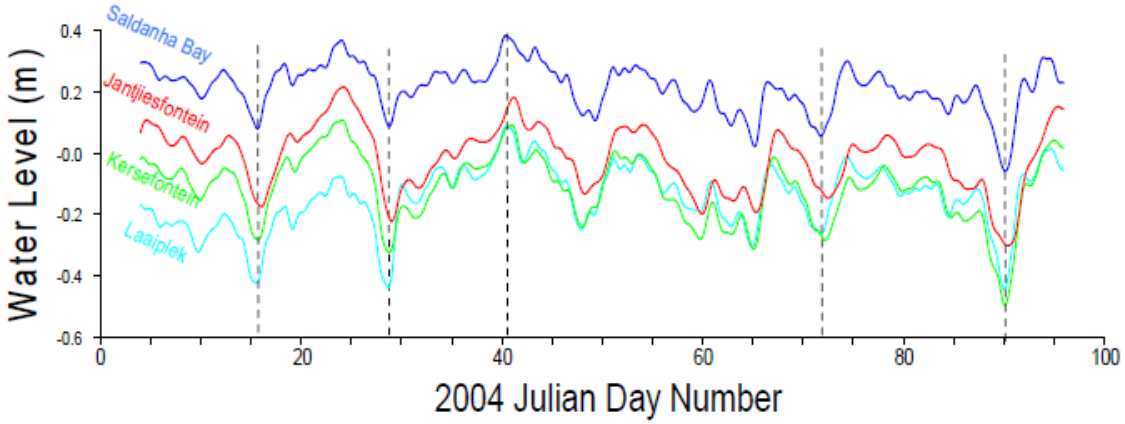

Figure 6.3 Longer-period water level variability at Saldanha Bay, Laaiplek, Kliphoek and Jantjiesfontein (Source: DWAF 2007)

The relative magnitude of tidal (derived from the more detailed CSIR 1990 water level measurements) and sub-tidal fluctuations on moving upstream in the estuary are plotted in Figure 6.4. These data indicate that the subtidal fluctuations under spring tide conditions only really dominate normal tidal water level variability upstream of Jantjiesfontein (> 50 km upstream). Under neap tide conditions, tidal water level variations are either on a par with or exceed subtidal

water level variation between Kliphoek and Kersefontein, depending on the magnitude of the subtidal water level variations. Only upstream of Jantjiesfontein does the magnitude of subtidal water level variability exceed that of normal tidal water level variations.

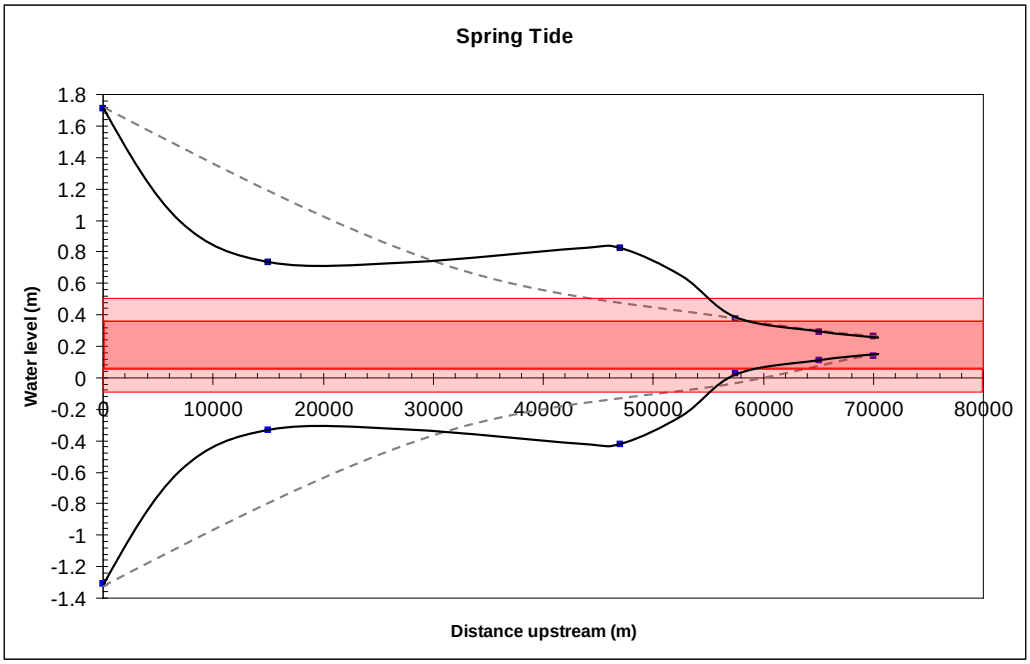

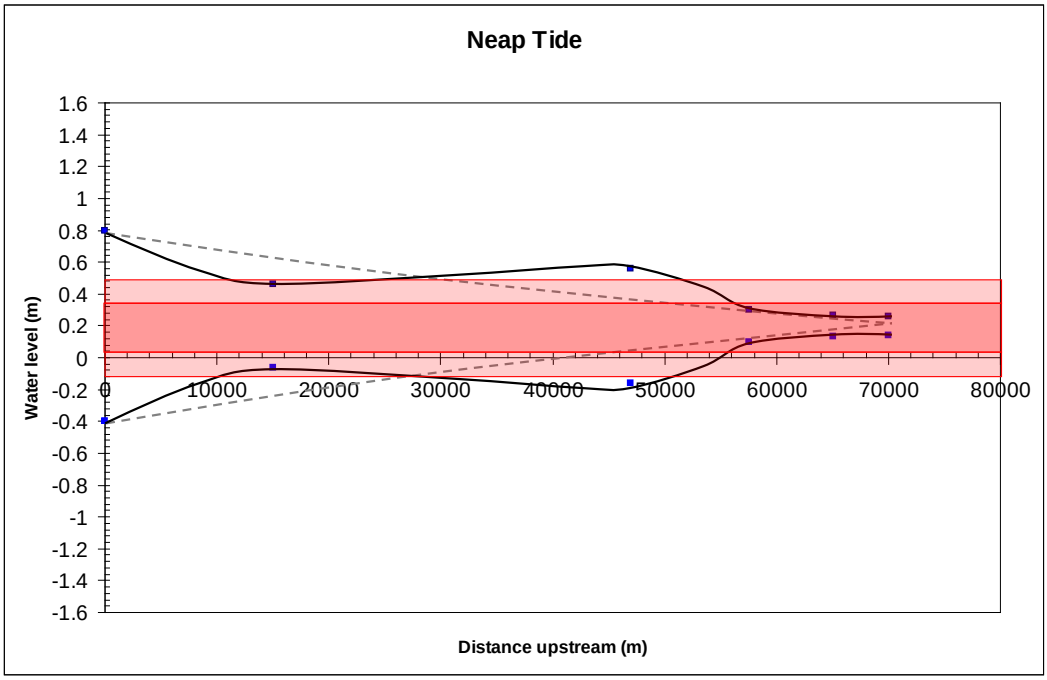

Figure 6.4 Water level variability plotted as a function of upstream distance. The lack solid line is the measured spring/neap tide tidal range, the dotted black line is the theoretical upstream decay in spring tide tidal range while the light red area denotes the likely extreme amplitude of subtidal fluctuations and the darker region the most likely range of subtidal fluctuations in water level.

6.1.3 Changes in upstream water levels due to freshwater inflows

The remaining driver of significant water level variability in the Berg River estuary is that due to freshwater inflows into the upper estuary. The magnitude of these increases in water level freshwater inflows are significant in the uppermost reaches of the estuary.

Measured data indicate that water levels in the upper reaches of the estuary increase with both increasing base flows as well as for freshettes and floods (Figure 6.5). The measured water levels at Jantjiesfontein and freshwater inflows to the estuary as reported by Beck and Basson (2007) show a clear relationship between water level and magnitude of winter baseflow. The water level at Jantjiesfontein increases more or less linearly with increasing freshwater inflows up to approximately 40 m^3/s. For freshwater inflows above 40 m^3/s the rate of increase in water level (measured at Jantjiesfontein) with increasing freshwater inflows begins to slow until, at freshwater inflows exceeding between 80 and 100 m^3/s, there is little or no increase in water level with increasing freshwater inflow. The reason for this is that the water level rises to such an extent for such higher flows that the estuary breaks its banks in these upper reaches and flows onto the adjacent flood plain.

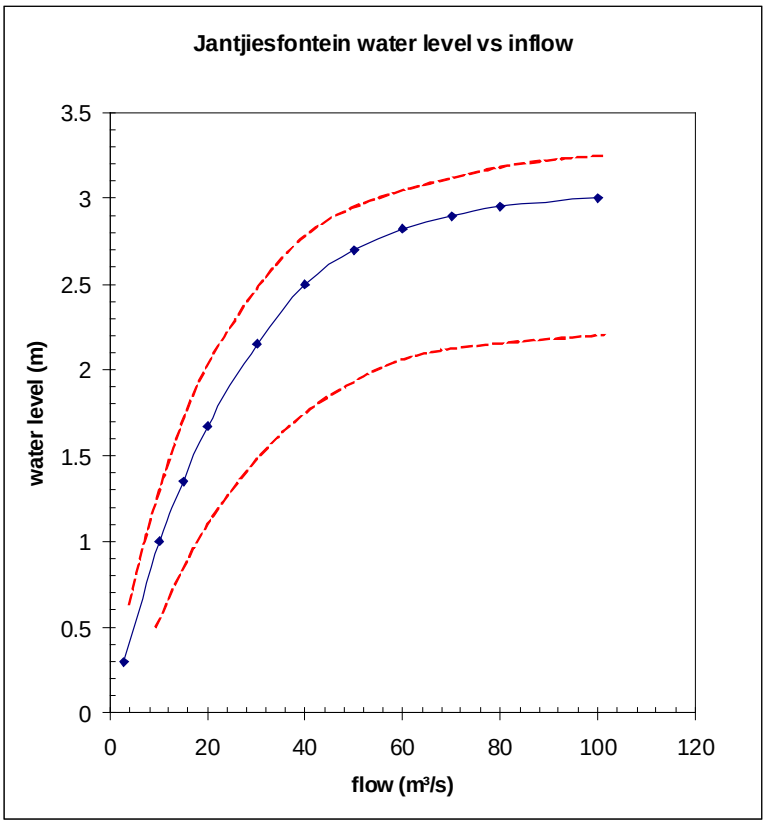

Figure 6.5 Schematic of the relationship between the measured water level at Jantjiesfontein and the estimated freshwater inflows to the estuary during the period Jan 1995 to November 2003.

What is not clear is how the water levels vary with changing base flow at other locations further downstream in the estuary. This change in water level (for changing winter base flows) upon moving downstream is important in characterising potential flooding associated with combinations base flows and flood sizes associated with past (natural), present (with Berg River dam) and potential future scenarios.

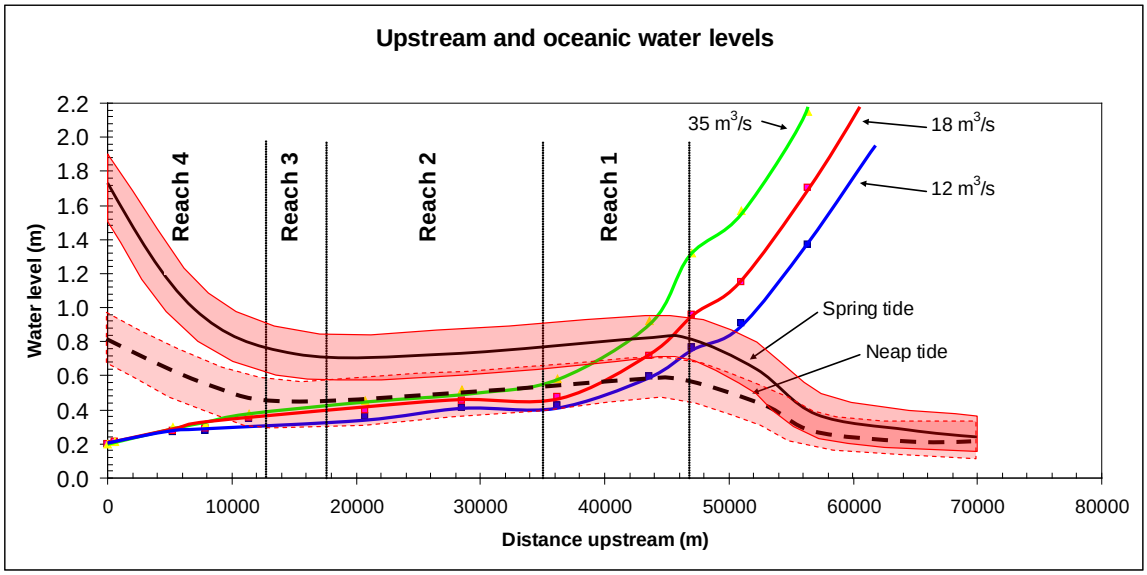

Figure 6.6 Schematic of the along estuary water level profile associated with various winter base flows. The shaded red area indicates typical sub-tidal variability around the normal spring and neap tide water levels. Overlaid are the spring and neap tide water level variations. The red shaded areas represent the range of possible variation in these tidal levels associated with typical subtidal water level variations in the adjacent ocean.

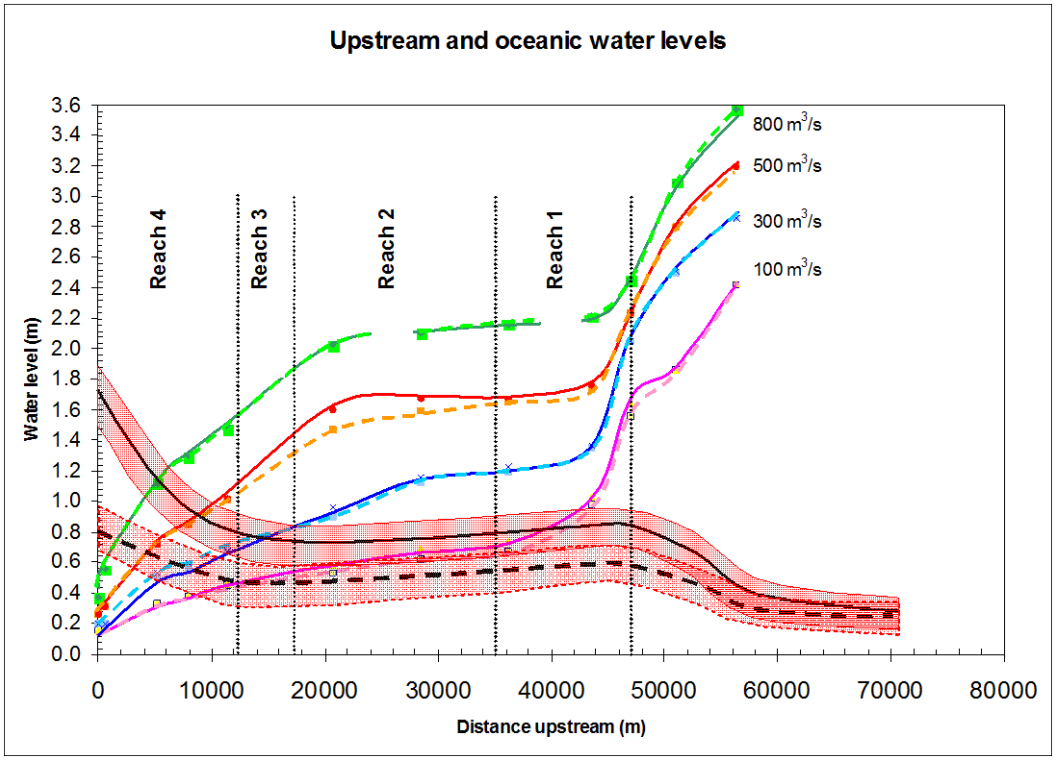

Figure 6.7 Schematic of the along estuary water level profile associated with various flood sizes under spring tide conditions. Overlaid are the spring and neap tide water level variations.

The downstream change in water level (with tidal fluctuations removed by filtering) associated with various winter base flows have been derived from the modelling studies as the distribution of the

DWAF water level gauges (see Figure 3.1) is such that they cannot resolve the downstream changes in water level associated with winter base flows.

There is a rapid decrease in water levels downstream of Rasgat. a "flattening of these water levels between Jantjiesfontein (~51 km upstream) and Kersefontein (~45 km upstream) and then a continued rapid decline in measured water levels until a location approximately 33 km upstream of the mouth (Figure 6.6). Downstream of this there is very little difference between the water level for winter baseline flows of between 35 m^3/s (natural winter baseflow conditions) and 12 m^3/s (winter base flow conditions under the more extreme development scenarios considered in this study). The implication is that variations in winter base flow are unlikely to influence significantly the flooding behaviour in the estuary downstream of flood Reach 1 (see Figure 6.8 for a description of the river reaches). The results in Figure 6.6 also suggest that upstream of 33 km from the mouth the effects of changes in winter base flows is likely to exceed those brought about by sub-tidal water level changes.

Maximum, modelled water levels along the axis of the estuary for various flood sizes are presented in Figure 6.7. These results suggest that freshettes and floods drive water level variations in Reaches 1 and 2 (and to a lesser extent Reach 3 depending on flood size). These results also suggest that only floods exceeding peak flows of 500 m^3/s will be clearly indentified in the measured water levels downstream of the Kliphoek water level gauge (i.e. downstream of the railway bridge).

6.1.4 In summary

Under normal (non-flood flow conditions) tidal water level variability dominates in the region between the mouth and 12 km upstream under neap tide conditions and up to between 45 and 50 km upstream under spring tide conditions. Upstream of this water levels are dominated by freshwater inflows should they be of any significance (*i.e*. winter base flows or greater). The magnitude of sub-tidal water level fluctuations is comparable to neap tide water level variations between 12 km and approximately 50 km upstream.

Depending on the magnitude and sign of subtidal water level variability, the magnitude tidal water level variability exceeds that associated with small floods (< 100 m^3/s) from the mouth to approximately 33 km to 45 km upstream for spring tides and from the mouth to approximately 20 km upstream under neap tides. For larger floods (> 500 m^3/s) tidal water level fluctuations only dominate downstream of approximately the railway bridge under spring tides and only in the lower 2 to 5 km of the estuary under neap tides. This is confirmed in the water level data measured at the DWAF water level gauge at Kliphoek.

The significance of the above observations is that past studies have suggested a very strong relationship between the extent of flooding and the magnitude of winter base flows (Beck and Basson, Ractliffe, 2009) as well as sub-tidal water level fluctuations at the mouth of the estuary. The present study (that took more explicit cognisance of the rapid downstream decrease in water level increases associated with winter base flows,) shows that there is only a weak relationship between base flow and the extent of flooding in all but most upstream reaches of the estuary and then only for smaller floods (< 200 m^3/s). Under small flood conditions (100 to 200 m^3/s) sub-tidal variability is expected to influence flood extents from the mouth to approximately 30 to 40 km upstream (depending on the magnitude of the subtidal water level fluctuations). Under large flood conditions it is expected that the influence of subtidal fluctuation will be limited to the region downstream of the railway bridge. Under non-flood conditions, sub-tidal water level variability is expected to significantly influence that area of the estuary where normal tidal water level variability dominates that associated with freshwater inflows, *i,e*, typically downstream of Kersefontein during

winter base flow conditions but as far upstream and Steenbokfontein (approximately 70 km upstream) during the low flow conditions of summer.

6.4 Hydrological Regime

The Berg River Estuary has a strongly seasonal hydrological regime. During winter, when the river is flowing strongly, the estuary is fluvially-dominated. Although saline intrusion occurs during flood tides, the system is usually flushed completely by river water during the subsequent ebb tide. River floods occasionally occur during the winter months. The extent of inundation of the flood plains adjacent to the estuary is determined by the severity of the flood (Huizinga *et al*., 1994; Berg, 1994).

During summer river inflow to the Berg River estuary is low and the system becomes marine dominated. The direct influence of flood tide seawater intrusion is typically confined to the reaches downstream of Kliphoek, (14 km from the mouth).

Longitudinal dispersion, due to diffusion effects from tidal mixing and velocity shear, drives the propagation of salt water upstream of the direct influence of seawater intrusion. These effects become significant under low flow conditions, i.e. summer. In the Berg River estuary the meandering channel occasions transverse velocity shear and the strong tidal influence contributes to upstream dispersion of salt water. Furthermore, persistent, high winds blow along the west coast during summer. Wind blowing along the surface of the estuary imparts momentum to the surface waters. Velocity differences between the surface and bottom waters (referred to as velocity shear) contribute to mixing in the system and the upstream propagation of salt water. As low flow conditions (resulting in increased tidal influence) persist, upstream salinities gradually increase. This upstream dispersion of salt water gradually results in the formation of a mass of characteristically estuarine water. This water is warmer than the seawater, cooler than the river water and has a salinity between that of sea water and fresh water (see chapter 7 for more detail). The plug of estuarine water undergoes limited renewal near the mouth during flood tidal intrusion. In systems, like the Berg River estuary, where salinity proceeds upstream by these mechanisms, the water column is generally vertically well mixed. As river flow decreases during summer, this saline water mass extends upstream until further progress is halted by the onset of the winter rains. The system then alters from vertically mixed to partially stratified conditions (Taljaard *et al*., 1992b).

A modelling study was undertaken as part of this study. In addition to using the modelling study to predict changes in salinity distributions in the Berg River in summer under various present and future flow scenarios (marine-dominated state); the hydrodynamic model simulations have

Table 6.5 Seasonal scenarios simulated to assess changes in salinity in the Berg River Estuary under reference, pre- and post-Berg River Dam and potential future flow conditions associated with proposed development options in the catchment.

Flow conditions	Summer base flow	Oct	Nov	Dec	Jan	Feb	Mar	Apr	May	Jun	Jul	Aug	Sept
Natural conditions (pre-development)													
Reference	(as estimated)	21.48	10.53	4.54	2.35	1.54	1.78	5.94	20.97	44.27	65.02	62.56	39.31
No Berg River Dam (conditions prior to the construction of the Berg River Dam)													
Pre- Berg River Dam	0.30 m3/s	11.12	5.07	0.30	0.30	0.30	0.30	1.99	11.40	22.96	35.69	36.79	23.48
	0.90 m3/s	11.12	5.07	0.90	0.90	0.90	0.90	1.99	11.40	22.96	35.69	36.79	23.48
	0.15 m3/s	11.12	5.07	0.15	0.15	0.15	0.15	1.99	11.40	22.96	35.69	36.79	23.48
Present conditions (conditions after the construction of the Berg River Dam)													
Present	0.30 m3/s	8.28	4.02	0.30	0.30	0.30	0.30	1.42	6.90	16.13	27.74	28.66	20.15
	0.90 m3/s	8.28	4.02	0.90	0.90	0.90	0.90	1.42	6.90	16.13	27.74	28.66	20.15
	0.15 m3/s	8.28	4.02	0.15	0.15	0.15	0.15	1.42	6.90	16.13	27.74	28.66	20.15
Raised Misverstand, Imposed resdss ifrD. Ifr = 15% of natural flow													
Possible “worst case”	0.30 m3/s	7.99	3.36	0.15	0.30	0.21	0.15	0.30	6.91	16.00	21.10	14.34	14.51
	0.90 m3/s	7.99	3.36	0.90	0.90	0.90	0.90	0.90	6.91	16.00	21.10	14.34	14.51
	0.15 m3/s	7.99	3.36	0.15	0.30	0.21	0.15	0.30	6.91	16.00	21.10	14.34	14.51
	0.00 m3/s	7.99	3.36	0.00	0.00	0.00	0.00	0.30	6.91	16.00	21.10	14.34	14.51

been used to better understand the dynamics of the Berg River estuary. In particular, a range of hydrodynamic simulations were designed to:

- describe the likely seasonal distributions of salinity under historical flow conditions (Reference and pre-Berg River Dam flow conditions), present day conditions and potential future conditions.
- gain an understanding of how easily salinity distributions are likely to change under various scenarios such as freshettes, small flood and extreme low flow conditions. Specifically the intention is to use shorter term model simulations to:
    - determine what magnitude of freshwater inflows are required to flush the Berg River estuary to 1/3 and 2/3 of its longitudinal extent at the end of summer (transition state);
    - determine the magnitude of freshwater spate or flood required for the Berg River estuary to become freshwater dominated.

The shorter-term model simulations indicated that:

- the salinity distribution in the reach upstream of 45 km was very sensitive to changes in summer base flows;
- freshwater spates of approximately 160 m^3/s would completely flush saline waters out of the estuary on the outgoing tide. This agrees with Schumann's observation that flows exceeding 140 m^3/s completely flush saline waters out of the estuary on the outgoing tide. Only the largest floods > 500 m3/s will create a freshwater plume sufficiently extensive to prevent the ingress of all but low salinity waters in the lower estuary with the incoming tide.

A series of longer-term simulations (based on monthly median freshwater inflows) have been undertaken to assess the changes in salinity distributions in the Berg River in late summer under historical, present and possible future conditions where the freshwater inflows (particularly the summer base flows) are reduced (see Table 6.5).

However, given the difficulty in accurately estimating freshwater inflows into the estuary under summer base flow conditions and the sensitivity of the upper reaches of the estuary to small changes in freshwater inflow, it was anticipated that it would be quite difficult to distinguish between future development scenarios based solely on the model simulations of salinity distributions.

The uncertainty in summer baseflows and the sensitivity to small changes in summer baseflows in the upper reaches resulted in a more extensive set of model simulations being undertaken than was originally anticipated. While the most likely summer base flow entering the estuary is expected to be in the range of 0.3 m^3/s (possibly due to reducing abstractions over weekends), it is possible for the baseflows to range between 0.15 m^3/s and 0.9 m^3/s. Consequently additional simulations were undertaken assuming a range of summer base flows comprising summer base flows of 0.9 m^3/s (base flow due to spillage over Misverstand), 0.15 m^3/s (assumed low base flow condition) and an extreme situation of 0.0 m^3/s.

Each run was started at the transition to the dry season (December).and run for 5 months (*i.e.* until the end of the dry season in April). As median monthly flows were used in the simulations, shorter term variability such as individual floods, etc could not be resolved. This was not considered problematic as the issue being investigated was the seasonal changes and the extremes of upstream salinity penetration in the upper reaches of the estuary under various historical, present and future flow conditions.

Due to the nature of the model set-ups the effects of evaporation were overestimated especially in the lower reaches of the estuary. Consequently only the salinity distributions upstream of approximately 25 km were considered robust enough upon which to base conclusions.

Time series of salinity were output for locations 0km, 6 km, 25 km, 33km, 45 km, 50 km and 57 km upstream of the mouth of the estuary.

The outcomes of the model simulations are as follows:

- Reference conditions
  - Saline waters rarely penetrated further than 25 km upstream at the end of the low flow season

- Pre-Berg River Dam
  - *Summer base flow = 0.15 m³/s*: At the end of the low flow season saline water (< 2 psu) penetrates as far as 50 km upstream, 21 psu is observed at 33 km upstream, 4 psu is observed at 45 km upstream
  - *Summer base flow* = 0.30 m³/s: At the end of the low flow season saline water (< 1 psu) penetrates as far as 45 km upstream and 14 psu is observed at 33 km upstream
  - *Summer base flow* = 0.90 m³/s: At the end of the low flow season saline water (< 2psu) penetrates beyond 33 km upstream but not as far as 45 km upstream

- Present Day (post Berg River Dam)
  - *Summer base flow* = 0.15 m³/s: At the end of the low flow season saline water (< 2 psu) penetrates as far as 50 km upstream, 24 psu is observed at 33 km upstream and 5 psu is observed at 45 km upstream
  - *Summer base flow* = 0.30 m³/s: At the end of the low flow season saline water (< 1 psu) penetrates as far as 45 km upstream and 16 psu is observed at 33 km upstream
  - *Summer base flow* = 0.90 m³/s: At the end of the low flow season saline water (< 3psu) penetrates beyond 33 km upstream but not as far as 45 km upstream
  - *Summer base flow* = 0.30 m³/s with sea level rise of 0.5m: At the end of the low flow season saline water (< 2 psu) penetrates as far as 50 km upstream, 26 psu is observed at 33 km upstream (This is similar to the salinity distribution for present day 0.15 m³/s flows, *i.e.* the assumed sea level rise 0.5 m is equivalent to a hhalving of the 0.3 m³/s summer base flow)

- Misverstand D (worst case)
  - *Summer base flow* = 0 m³/s: At the end of the low flow season saline water (< 2 psu) penetrates as far as 57 km upstream, 30 psu[2] (?) observed at 33 km upstream, 9 psu observed at 45 km upstream, 5 psu observed at 50 km upstream
  - *Summer base flow* = 0.15 m³/s: saline water (< 2 psu) penetrate as far as 50 km upstream, 25 psu observed at 33 km upstream, 6 psu observed at 45 km upstream
  - *Summer base flow* = 0.30 m³/s: start to see evidence of saline water (> 0 psu) at 50 km, saline water (< 2 psu) penetrates as far as 45 km upstream, 20 psu observed at 33 km upstream
  - *Summer base flow* = 0.90 m³/s: saline water (< 4psu) penetrates beyond 33 km upstream but not as far as 45 km upstream
  - *Summer base flow* = 0.30 m³/s with sea level rise of 0.5m: not simulated

6.4 Flood Regime

The flood regimes considered in this study (Figure 6.8) are those originally defined by Beck and Basson (2007) in their modelling study for the Berg River Baseline monitoring programme. These studies showed the flooding regime to be significantly influenced by upstream water levels at the start of a flooding sequence (that are closely related to winter base flow) as well as sub-tidal water level fluctuations at the mouth of the estuary (Beck and Basson (2007).

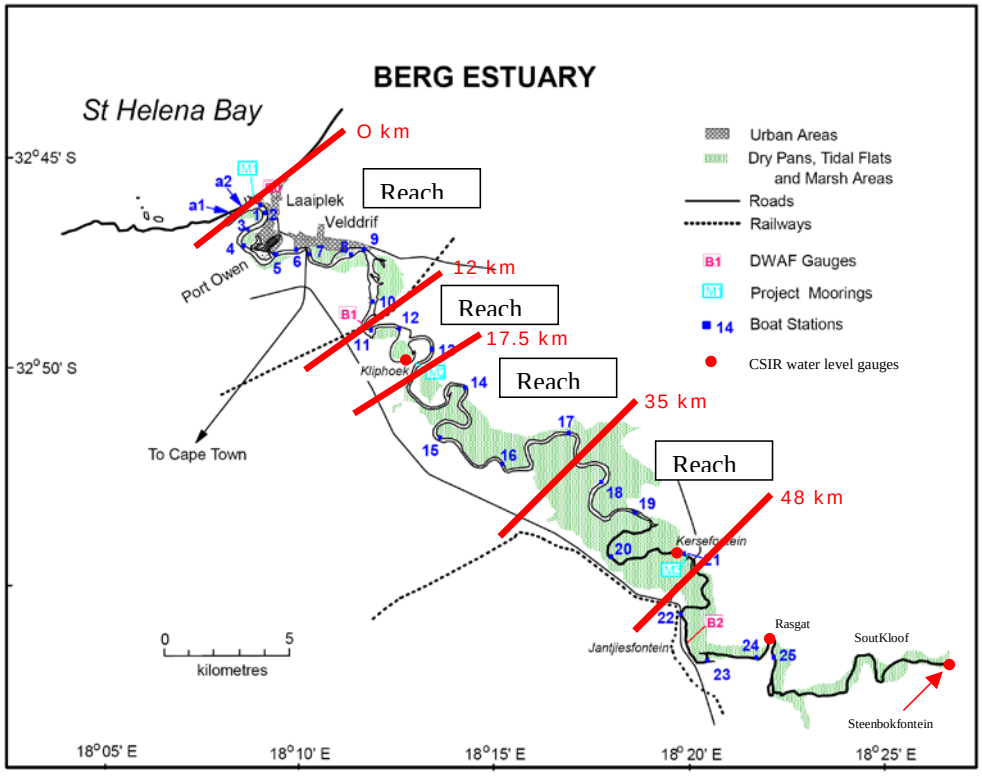

Figure 6.8 Flood zones defined for the Berg River Baseline Modelling Studies (Beck and Basson. 2007).

[2] Given the errors introduced by the effective "overestimation" of evaporative effects (associated with exact nature of the model set-ups), there is considerable uncertainty around this figure.

A flood modelling study was undertaken (See Annex 1) whereby flood simulations were undertaken for a range of flood events have been assessed under two winter "base flow" scenarios. Originally three categories of winter base flows were assumed;

I. Winter base flows > 30 m^3/s representing reference conditions
II. Winter base flows ranging between 15 and > 30 m^3/s representing conditions before the building of the Berg River Dam
III. Winter base flows < 15 m^3/s representing encompassing present conditions, as well as all of the future scenarios proposed for this study.

These winter base flows represent upstream water elevations at Jantjiesfontein of 2.3 m, 1.6 m and 1.2 m, respectively.

Based on these winter base flow categories, the likely maximum flood extents and durations of inundation of various locations can be assessed for a range of historical, present and possible future flow conditions in the Berg River estuary. The flood sizes considered were 100 m^3/s, 200m^3/s, 300m^3/s, 400 m^3.s, 500m^3/s, 600m^3/s, 800 m^3/s and 1000 m^3/s. Examples of the results of the flood modelling study are given in Figure 6.9 to Figure 6.11.

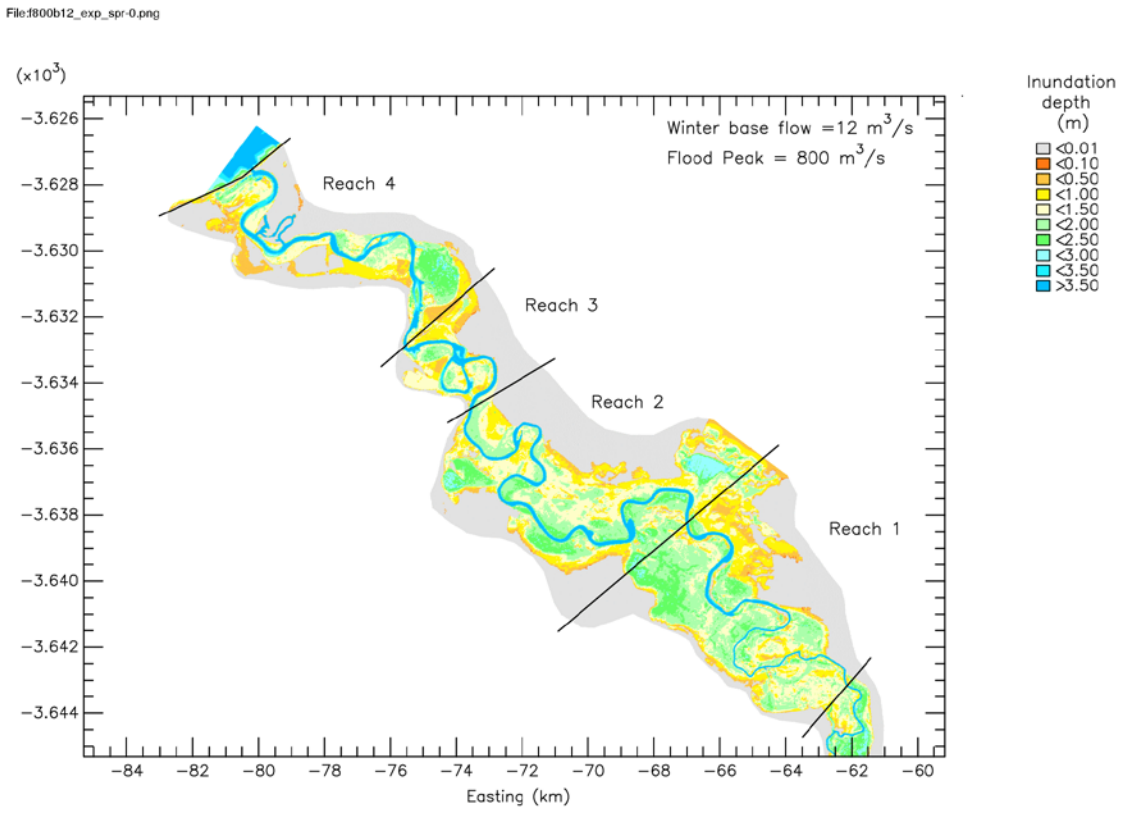

Figure 6.9 Flood extent for an 800 m^3/s flood under present day base flow conditions

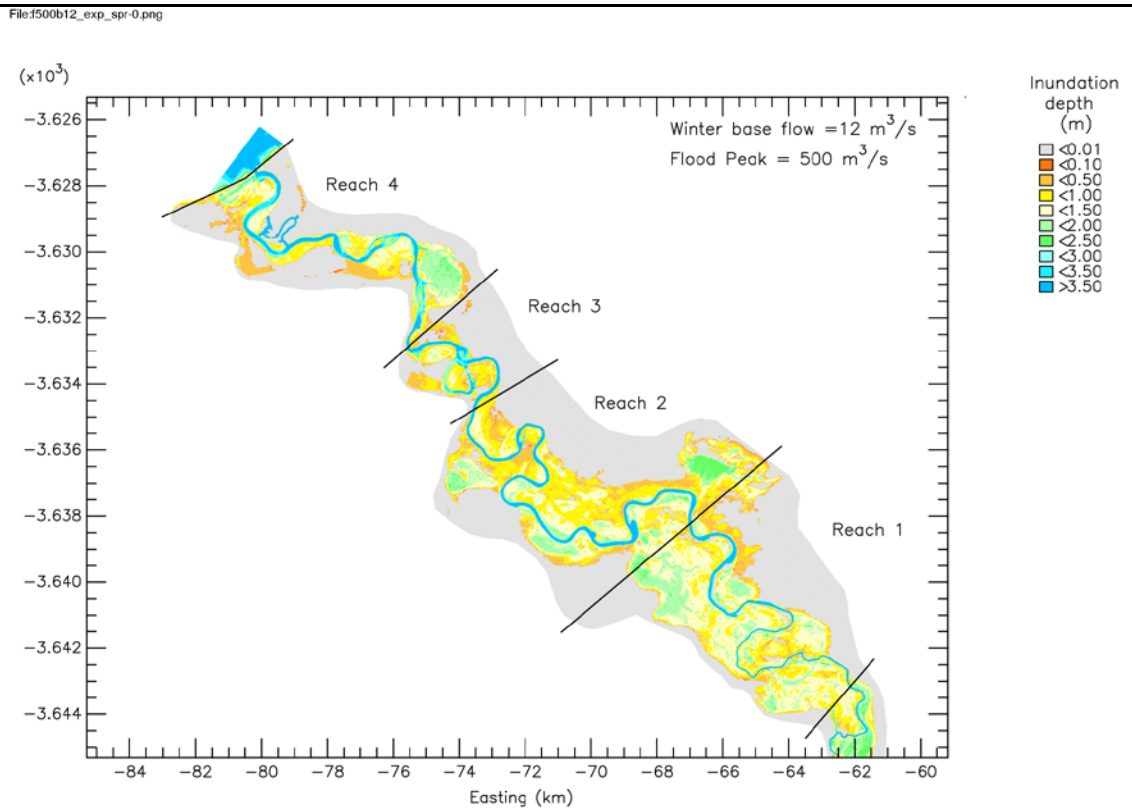

Figure 6.10 Flood extent for a 500 m^3/s flood under present day base flow conditions

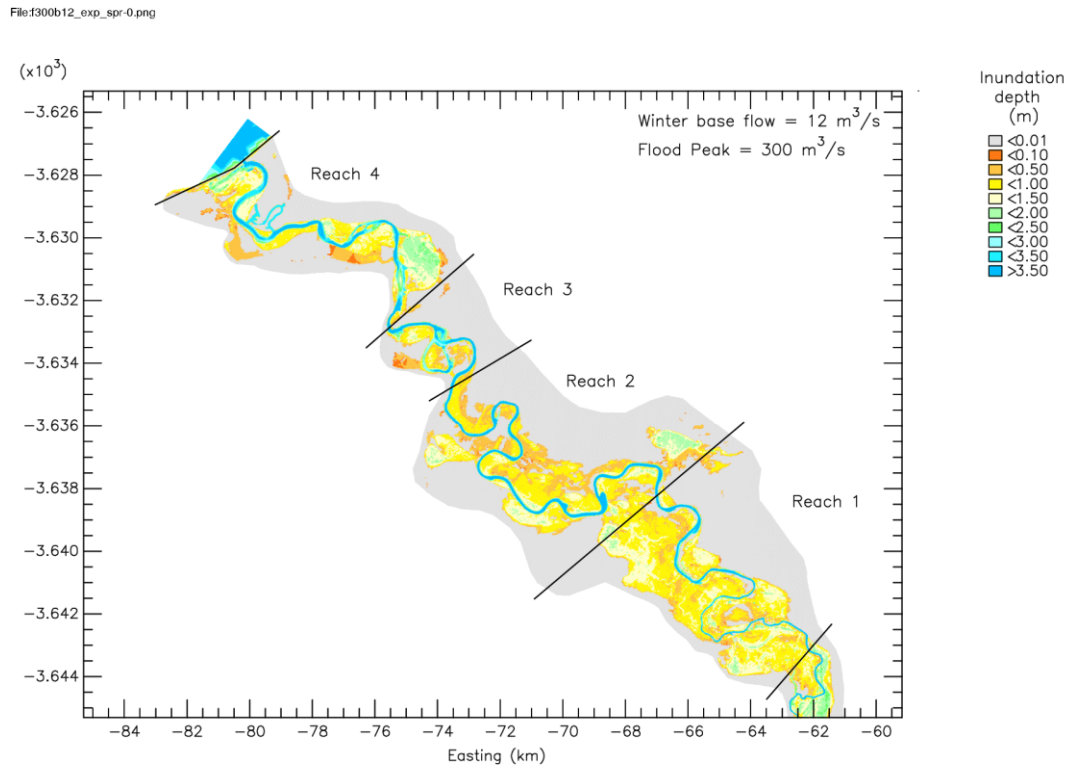

Figure 6.11 Flood extent for a 300 m^3/s flood under present day base flow conditions

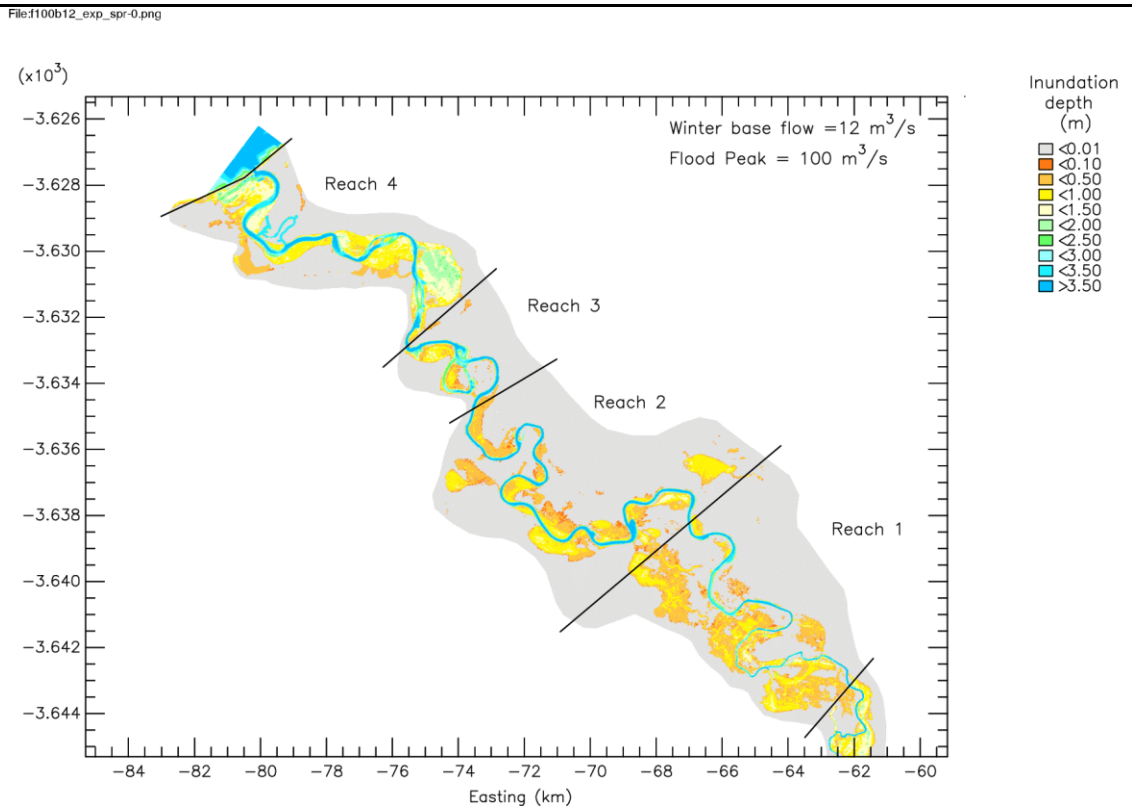

Figure 6.12 Flood extent for a 100 m3/s flood under present day base flow conditions

Analysis of both measured and modelled water levels confirmed that the effect of upstream water level (*i.e*. magnitude of winter base flows) was overemphasised. There is only an approximate 2 to 3 % change in flood extent between the same size floods for winter base flows for the reference conditions (35 m^3/s) and those that typically expected to occur for the proposed new development scenarios (12 m^3/s). Tabulated results clearly indicate that this difference is small (compare Table 6.6a and b). Similarly the influence of sub-tidal water levels on the flood extents is not universal throughout estuary although the water level changes due to sub-tidal water variability at the mouth of the estuary are observed to be unattenuated throughout the estuary. Of equal significance to that of subtidal sea level variability is whether the flooding occurs during spring or neap tide conditions, particularly in the lower to middle reaches where tidal variability remains significant.

The spatial extent of pans that remain after flood events and the duration of such inundation is important to particularly the vegetation and avifauna in the Berg River estuary.

In the flood modelling study pans were broadly identified as depressions that would fill when flooded by would not completely drain once the floodwaters had receded. This identification was based on the time series results of Beck and Basson and a rough confirmation of the pans identified was undertaken. The spatial area of each pan was obtained from data used in the Berg River Baseline Monitoring Study (DWAF, 2007). The sites condsidered to represent areas of special interest in the Berg River Baseline Monitoring Study (and from which potential pan sites were selected for this study) are indicated in Figure 6.13. This more mechanistic definition of a pan does not necessarily represent a specific ecological functionality as defined in the vegetation and avifauna specialist studies. Additional effort is required to provide a collective flooding index for pans with a specific ecological function. The results in Table 6.6 and Table 6.7 should therefore

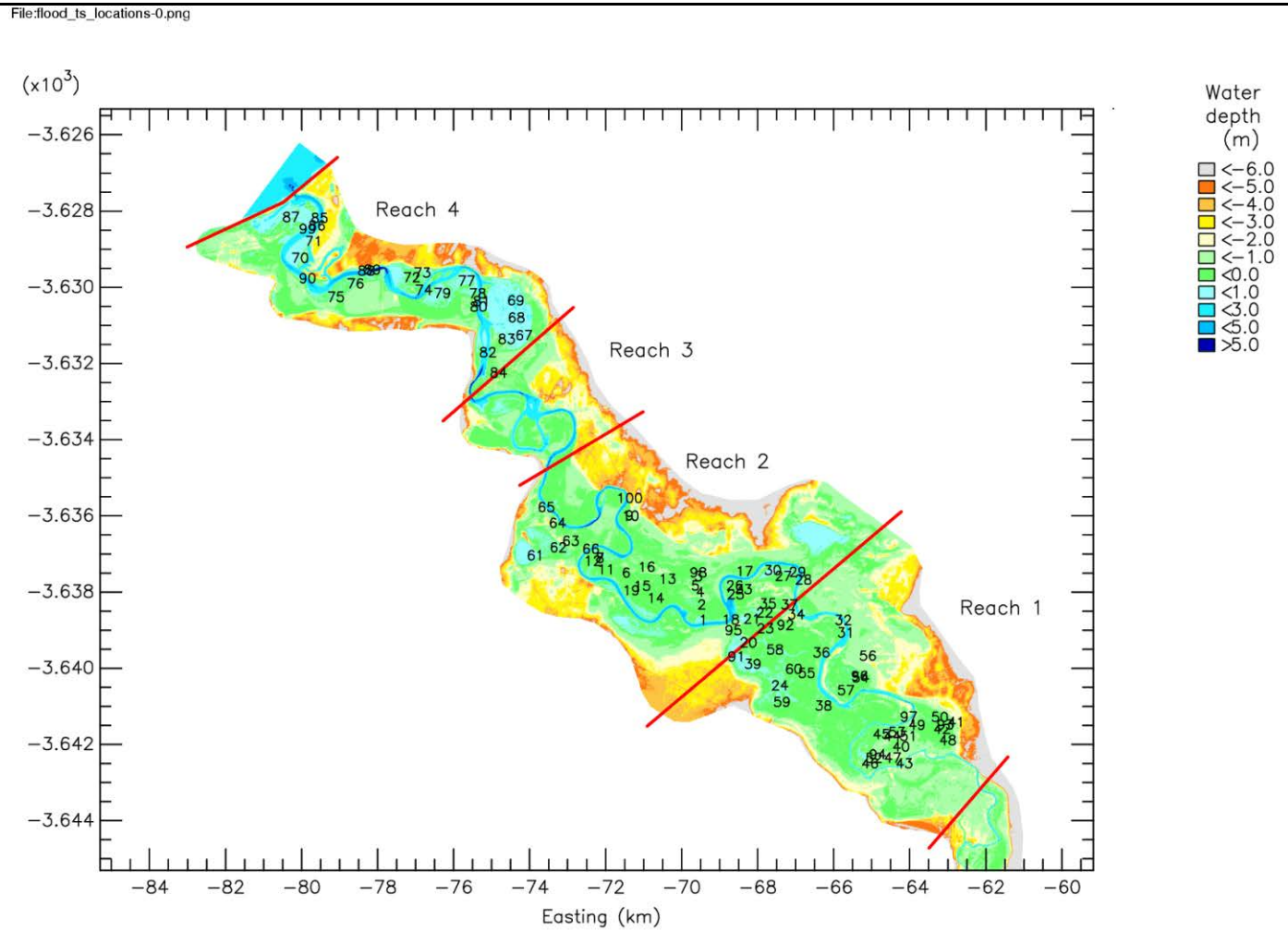

Figure 6.13 Sites identified in the Berg River Baseline Monitoring as of special interest, which were used to identify pans of relevance in the flood modelling study

Table 6.6 Flood extents of flood plain and pans for a range of flood sizes under reference condition winter base flows (35 m3/s)

Peak	Volume	Winter Baseflow			Flood Peak			Pans, marshes and inundated mudflats				
		Area	Area	Duration	Area	Area	Duration	Area	Area	% area remaining 30 days	% area remaining 60 days	% area remaining 120 days
m³/s	M m³	ha	%	days	ha	%	days	ha	%			
1000	257	2557.4	36.9	90	6927.9	100.0	10 - 20	1088.4	100.0	84.0	71.6	31.2
800	203	2557.4	36.9	90	6692.4	96.6	10 - 20	1088.4	100.0	84.0	71.6	31.2
600	149	2557.4	36.9	90	6149.6	88.8	10 - 15	1088.4	100.0	84.0	71.6	31.2
500	125	2557.4	36.9	90	5810.1	83.9	10- 14	1088.4	100.0	84.0	71.6	31.2
400	96	2557.4	36.9	90	5471.1	79.0	7 - 14	1088.4	100.0	84.0	71.6	31.2
300	65	2557.4	36.9	90	5000.8	72.2	7 - 10	942.9	86.6	70.9	59.2	22.4
200	42	2557.4	36.9	90	4457.1	62.7	5 - 10	923.2	84.8	69.2	57.9	22.4
100	15	2557.4	36.9	90	3789.4	54.7	5 - 7	783.0	71.9	56.9	47.3	18.1

Table 6.7 Flood extents of flood plain and pans for a range of flood sizes under future scenario winter base flows (12 m^3/s)

Peak	Volume	Winter Baseflow			Flood Peak			Pans, marshes and inundated mudflats				
		Area	Area	Duration	Area	Area	Duration	Area	Area	% area remaining 30 days	% area remaining 60 days	% area remaining 120 days
m³/s	M m³	ha	%	days	ha	%	days	ha	%			
1000	257	2407.2	34.7	90	6827.4	98.5	10 - 20	1088.4	100.0	83.9	71.5	31.2
800	203	2407.2	34.7	90	6684.2	96.5	10 - 20	1088.4	100.0	83.9	71.5	31.2
600	149	2407.2	34.7	90	6105.2	88.1	10 - 15	1088.4	100.0	83.9	71.5	31.2
500	125	2407.2	34.7	90	5759.3	83.1	10- 14	1088.4	100.0	83.9	71.5	31.2
400	96	2406.9	34.7	90	5393.1	77.8	7 - 14	1088.4	100.0	83.9	71.5	31.2
300	65	2407.2	34.7	90	4901.3	70.7	7 - 10	942.9	86.6	70.9	59.2	22.4
200	42	2406.9	34.7	90	4329.5	62.5	5 - 10	923.2	84.8	69.2	57.8	22.4
100	15	2407.2	34.7	90	3521.1	50.8	5 - 7	783.0	71.9	56.9	47.3	18.1

* The percentage area of inundated flood plain is normalised to the maximum flooded area under the maximum flood conditions simulated (*i.e.* 1 000 m^3/s)

* The percentage area of inundated flood plain is normalised to the possible flooded pan area of the pans under consideration.

be considered as indicative rather than definitive. Also tabulated are the spatial extents of pans area that remain inundated after specific time periods.

While the magnitude of evaporation effects is irrelevant to areas that are drained after a flood event, evaporation effects are important in the pans. Each pan when filled has a characteristic depth and spatial extent that would decrease over time due to evaporation. This rate of evaporation and resultant change in water depth and extent of the pan is unique to each pan. In the modelling studies we have assumed that evaporation is the only factor reducing water depth of these pans (*i.e*. no loss of water due to seepage). The long-term evaporative effects therefore estimated by reducing the water level in each pan under consideration by the net expected water loss (evaporation – rainfall) for the months of August to November. The 1 August was the assumed start date from which evaporative effects were considered, *i.e.* the assumption being that the pans had been flooded towards the end of the high flow season. This provides a "worst case" scenario for the drying out of pans after flooding. During the wet season it is expected that the pans would be flooded on a number of occasions.

The maximum pan area inundated under each flood scenario (i.e. combination of winter base flow and flood size) was estimated for each of the four river reaches. Also estimated was the rate at which the pans area decreased due to evaporation. Estimated pan areas were estimated at 30 days after the flood event, 60 days after the flood event and 120 days after the flood event. These pan areas are only valid under the assumption that no further flood events occurred after the initial flood event. This idealised approach is an extremely conservative approach as in reality further flood events may well have occurred and filled one, more or all of the pans.

Differentiating between the various proposed future scenarios in terms of changes in flooding extents therefore cannot be done on changes in winter base flow. Rather it is the change in flood size, timing and number of flood events in each flood size class that determine the regularity and extent of flooding of both the flood plain and its associated pans.

Table 6.8 depicts the occurrence of floods in the Berg Estuary under the present conditions based on simulated monthly data. The flood analyses were based on an average winter baseflow of about 12m^3/s, *i.e.* low winter base flow conditions representing present day flow conditions. About 82% of the floods experience under the present conditions occurr between June and September, with 24% of these occuring in August. Presently the floodplain experiences some inundation for 30% of the months within a year. For about 4 % of the months in the 77-year simulation period based on present day conditions, floods will inundate between 90 to 100% of the floodplain. Similarly for about 3% of the months floods will inundate between 80 and 90% of the floodplain. While between 70 and 80% of the floodplain will be inundated in ~ 7% of the months in the simulation period. Between 50 and 70% of the flood plain will be inundated for about 16 % of the months. These lower levels of inundation are caused by floods with flood peaks between 100 to 300 m^3/s. These size classes of floods are relatively sensitive to setup in the preceding flood volumes, *i.e*. whether they are coming through as a single event or as a combination of pulses. The latter can increase the level of inundation significantly, *e.g*. from 50% to 60%. Water resources development in the catchment will have the effect of reducing complex flood patterns to short, sharp pulses.

It should be noted that under present day conditions that the base flows occurring between June and July will on average inundate about 34.7% of the floodplain. Under reference conditions there

was an approximate 2 % greater inundation, mostly in the upper reaches of the estuary (Flood Reach 1).

Table 6.8 Occurrence of floods and extend of floodplain inundation under the Present State based on simulated monthly flow data for a 77-year period

Flood Peak (m^3/s)	Area (ha)	No of floods in month during simulated 77 year period												% Occurrence/ flood size class	% inundation	% Occurrence/
		Oct	Nov	Dec	Jan	Feb	Mar	Apr	May	Jun	Jul	Aug	Sep			
100-200	3521.1	11	3	2	0	0	1	3	8	17	18	20	24	12	50-70	16
200-300	4329.5	3	1	0	0	0	0	0	2	2	10	9	9	4		
300-400	4901.3	3	1	0	0	0	0	1	4	11	7	6	11	5	70-80	7
400-500	5393.1	2	0	0	0	0	0	0	1	2	8	7	3	2		
500-600	5759.3	0	0	0	0	0	0	0	2	2	4	2	1	1	80-90	3
600-800	6105.2	0	0	0	0	0	0	0	0	4	4	5	2	2		
800-1000	6684.2	0	0	0	0	0	0	0	1	1	0	5	2	1	>90%	4
>1000	6827.4	0	0	0	0	0	0	0	0	3	11	12	3	3		
Annual % occurrence		7	2	1	0	0	0	1	7	15	23	24	20			30

7 Water Quality

To assess changes in water quality, typical water quality characteristics associated with each of the abiotic states were derived, based on available data and information presented in the Berg River Baseline Monitoring Programme Report (Schumann, 2007; Clark and Taljaard, 2007).

The water quality characteristics of the different abiotic states are described in terms of the following parameters:

- Salinity
- Temperature
- pH
- Dissolved oxygen
- Secchi depth (transparency)
- Dissolved inorganic nutrients (dissolved inorganic nitrogen [DIN], dissolved inorganic phosphate [DIP] and reactive silicate).

To described the quality of river inflow to the estuary, data from the DWAF water quality monitoring station at Misverstand - Die Brug (G1H031Q01) and the Berg River Monitoring (BRM) Site 6 (at the N7 bridge - Piketberg) were used (Day, 2007). These sites are the most downstream sampling stations on the Berg River located above the head of the estuary. Day (2007) noted that there are no water quality records for the Berg River in an unimpacted state (reference condition). However, based on the catchment geology and the earliest data that are available, the river can be characterised in its upper reaches by naturally acid, low-nutrient, low conductivity waters. These characteristics altered with distance downstream, being highly dependent on both the underlying geology and flow conditions. Therefore even under the reference condition, the river would have shown a strong trend of increasing conductivity, increasing nutrients and increasing pH with distance downstream.

No recent data were available on toxic substance accumulation in the Great Berg Estuary. However, given the strong influence of agriculture in the catchment, the use of pesticides is assumed to be widespread and the likelihood of pesticide-contaminated runoff reaching the estuary is high. Also, the fishing harbour and marina in the lower reaches of the estuary is likely to introduce some trace metal and hydrocarbon pollutants into the system.

7.1 Temperature

Schumann (2007) illustrated typical seasonal distributions of temperature in the Great Berg Estuary (Figure 7.1) primarily based on measurements collected during the period 2002 to 2005.

Temperature in the Great Berg Estuary shows a distinct seasonal dependence (Schumann, 2007) (Figure 7.1), following air temperature over periods of days, where warmer days will mean a general increase in water temperatures, and colder days to a corresponding decrease. Summer insolation has a marked influence on the upper reaches of the estuary, the effect becoming apparent in early summer (November) and reaching a maximum in late summer (February) when maximum temperatures reached almost 28 ^{0}C. Summer upwelling results in the marked temperature variation in the lower reaches (Zones A and B) introducing cold seawater with temperatures as low as 13 ^{0}C. Higher temperatures in this area (> 20 ^{0}C) are associated with

down-welling. As winter approaches (May) water temperatures of inflowing river water also decrease (~18 ^{0}C).

Compared with summer, when variability in temperatures (13 – 28 ^{0}C) over the entire estuary can be as high as 15 ^{0}C, winter variability (12 – 18 ^{0}C) is typically 5 ^{0}C or less.

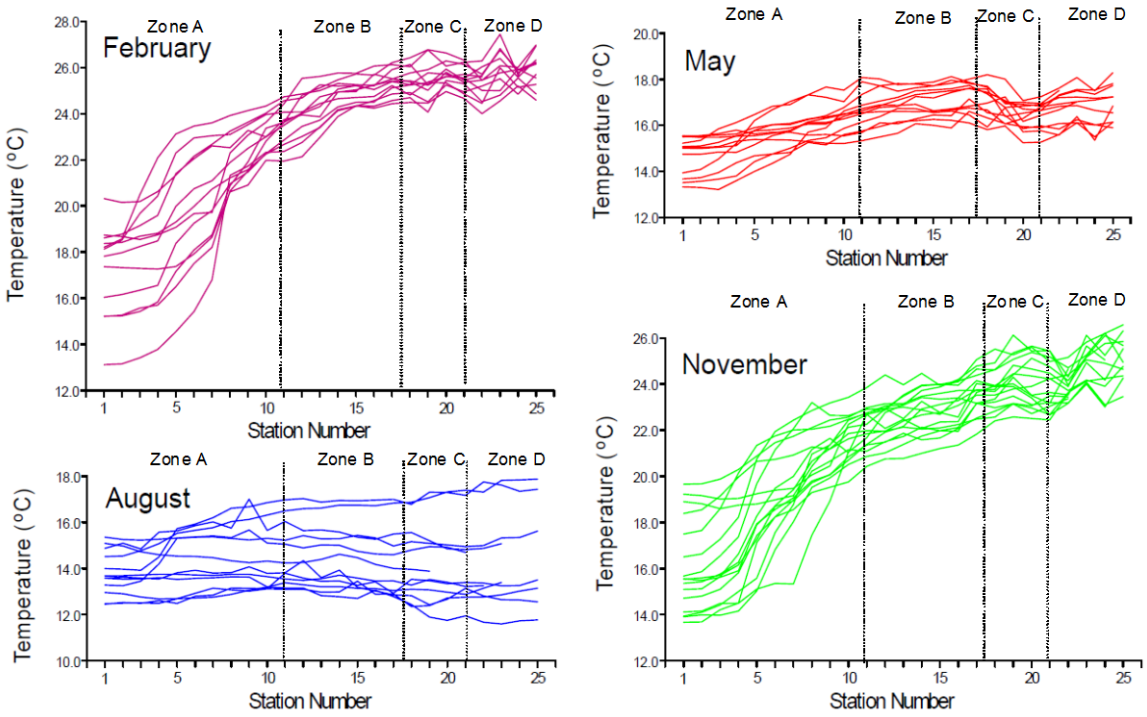

Figure 7.1 Vertically-integrated temperature distribution in the Great Berg Estuary (Schumann, 2007). Also indicated on the graphs are the different abiotic zone (Figure 5.1)

Based on the above, typical temperature distributions for the different abiotic states are as follows:

<u>State 1: Severe marine dominated & State 2: Marine dominated</u>

These states typically occur in summer when temperature variation along the length of the estuary can be high (~15^{0}C). The influence of cold, upwelled waters (when present) generally extend into Zones A and B, while temperatures in Zones C and D are largely reflects by atmospheric temperature.

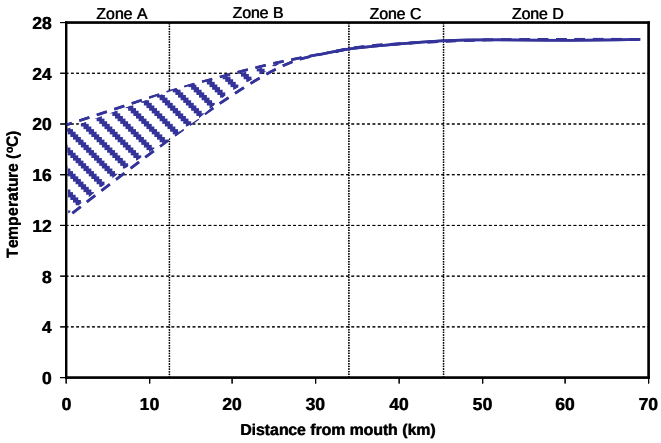

State 3: Small to Medium Freshwater inflow

This state generally occurs during autumn/spring, when temperature variation along the length of the estuary (~10^{0}C) is expected to be less severe than during summer. The influence of cold, upwelled water (when present) could still extend into Zones A and B, while temperatures in Zones C and D largely reflects atmospheric temperature or that of the inflowing river water.

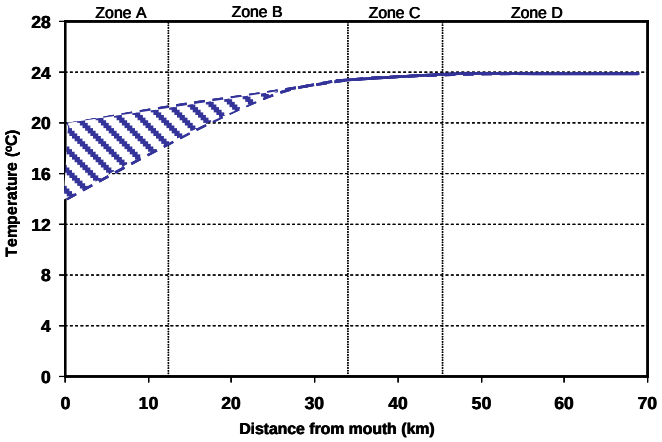

State 4: Medium to high freshwater inflow &State 5: Freshwater-dominated

This state is typical of the wetter, winter period when temperature variation along the length of the estuary is expected to be relatively small (~5^{0}C). Temperature throughout the estuary is largely reflect atmospheric temperatures or that of the inflowing river water.

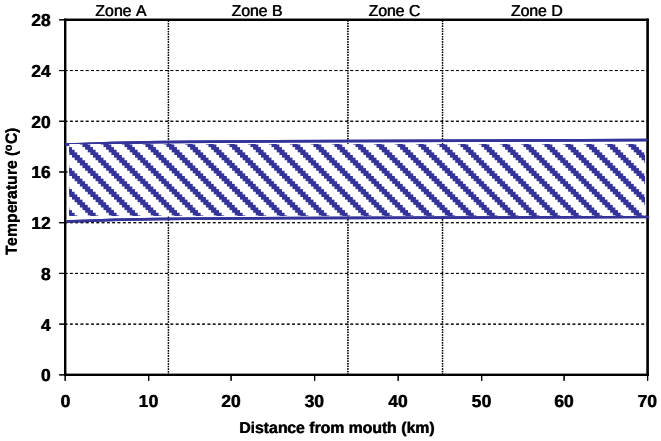

7.2 Salinity

Day (2007) concluded that conductivity increased substantially at all sites in the Berg River, and particularly in the lower reaches of the Berg since 1950 (~30 mS/m). These increases were primarily the result of increases in saline return flows from irrigation, coupled with abstraction of water from the main channel and its less saline tributaries. From 2003 to 2005 average measurements at BRM6 (N7 Bridge at Picketberg) were ~300 mS/m (summer and winter).

Schumann (2007) showed typical seasonal distributions of salinity in the Great Berg Estuary (Figure 7.2) primarily based on quarterly measurements collected during the period 2002 to 2005. Similar seasonal distributions were also observed in earlier studies (e.g. Taljaard et al, 1992; Slinger and Taljaard, 1996; Slinger et al, 1996).

Schumann (2007) concluded that for the most part, the Great Berg Estuary was well-mixed. Stratification seldom occurred, and did not seem to last very long, probably because of strong mixing from tidal exchange and fresh water inflow. It was therefore considered appropriate to integrate salinity and other water quality data over water depth at each station, using a mean value for each station (Figure 7.3).

Salinity structure in the Great Berg Estuary shows distinct longitudinal seasonal distribution patterns, largely driven by the extent of freshwater inflow, i.e. the extent of saline intrusion decreases with an increase in freshwater inflow. For example, during the dry season (February), saline waters penetrated well into Zone C, while in the wet season (August), strong freshwater influence limits saline intrusion to the lower sections of Zone A.

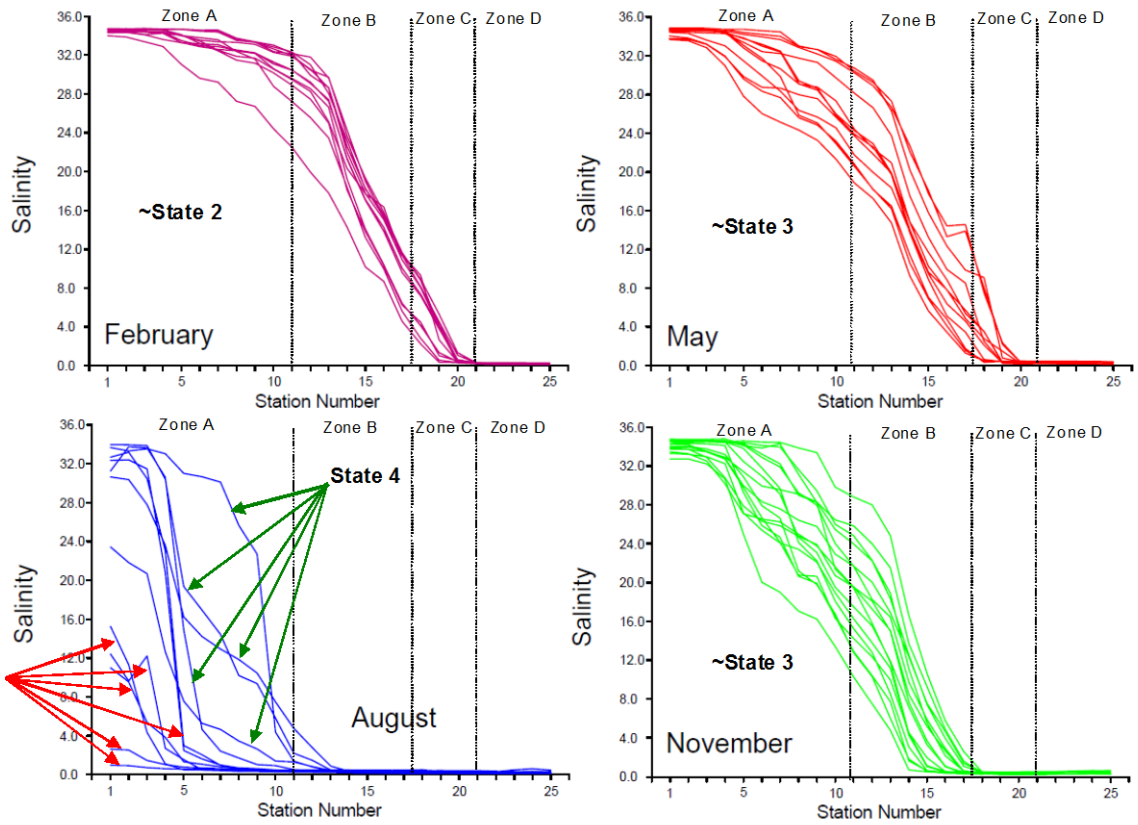

Figure 7.2 Vertically-integrated salinity distribution in the Great Berg Estuary from 2003 to 2005 (Schumann, 2007). Also indicated on the graphs are the different abiotic zone (Figure 5.1) and abiotic states considered representative of a particualr seasonal distribution

Using the above information, typical salinity distribution patterns for each of the five abiotic states are as follows:

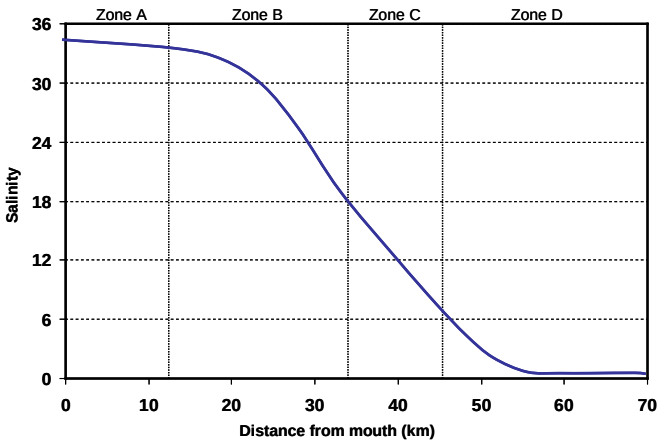

<u>State 1: Severe marine dominated</u>

During this state marine influence extends further than 45 km upstream of mouth (i.e. into Zone D) as a result of extended period of low or no river inflows. Zone A, possible lower section of Zone B are subject to frequent tidal flushing (this state not typical for reference condition or Present State, but possibly introduced in some of the Future Scenarios).

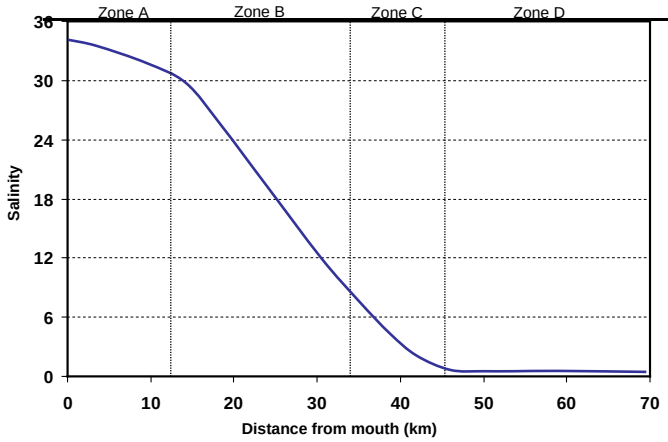

State 2: Marine dominated

During this state marine influence extends into Zone C, but not into zone D. Zone A is subject to frequent tidal flushing (this state is typical of the dry season under the Present State but not the reference condition)

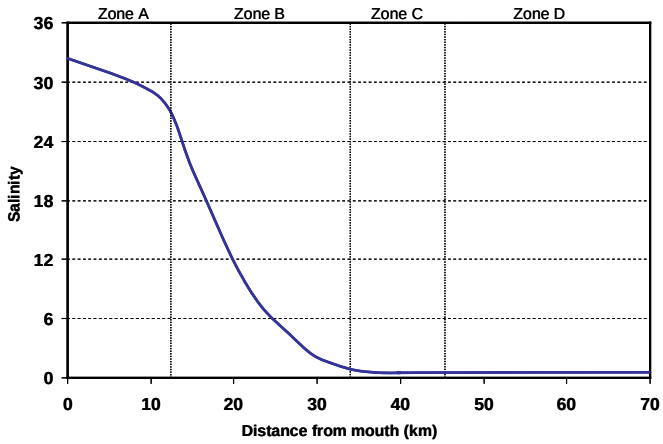

State 3: Small to Medium Freshwater inflow

During this state marine influence extends into Zone B, but not into Zones C and D (i.e. marine influence is only evident up to 33 km from mouth). Zone A is subject to frequent tidal flushing. There is strong freshwater influence in the upper ~40 km of the estuary (i.e. in Zones C and D) (typical of transition flows between wet and dry seasons and most likely during the dry season of the reference condition).

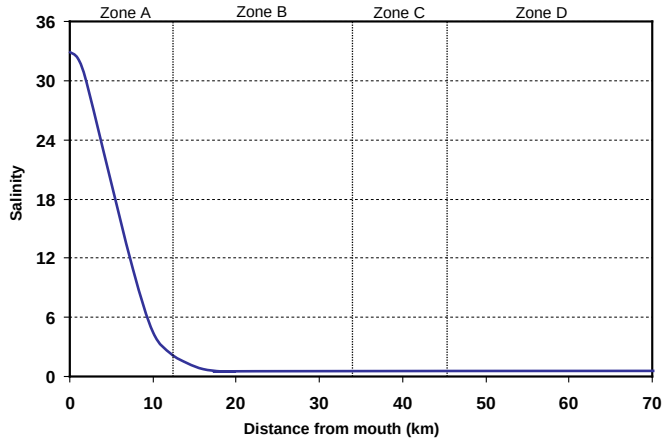

State 4: Medium to high freshwater inflow

During this state marine influence is only evident up to 12 km from mouth (i.e. downstream of Zone B), with strong freshwater influence in the upper ~60 km of the estuary (i.e. in Zones B-D) (typical of transition flows between wet and dry seasons).

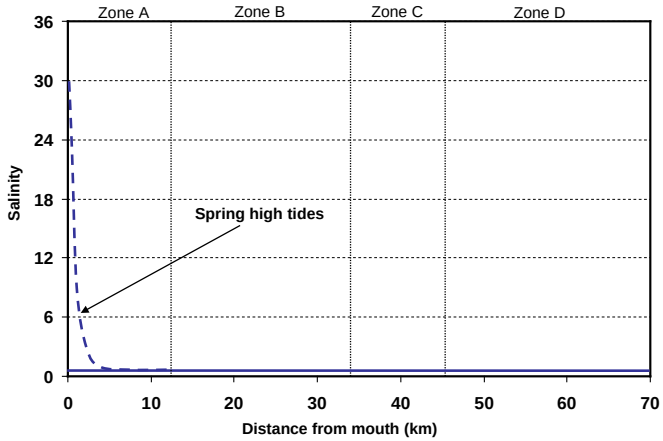

State 5: Freshwater-dominated

During this state the estuary is completely fresh (i.e. Zones A-D), except during spring high tides when seawater intrusion may occur into the lower 6 km of the estuary (Zone A) (typically occurring during high flow periods in the wet season).

7.3 pH

Based on data collected during 2003-2005 (Day, 20070 pH data in the upper reaches of the Berg River were still representative of acid mountain streams in the Cape fynbos region, despite impacts in the form of afforestation and clearing of forested areas. pH values increased markedly with distance downstream. However, based on the catchment geology, the river would have shown a strong trend of increasing increasing pH with distance downstream. pH measurements collected at Misverstand (Die Brug - G1H031Q01) since 1990 is provided in Figure 7.3. Results show that pH levels generally fall between 7 and 8.4. Day (2007) observed slight peaks in during spring at BRM 6 probably linked to particular farming activities.

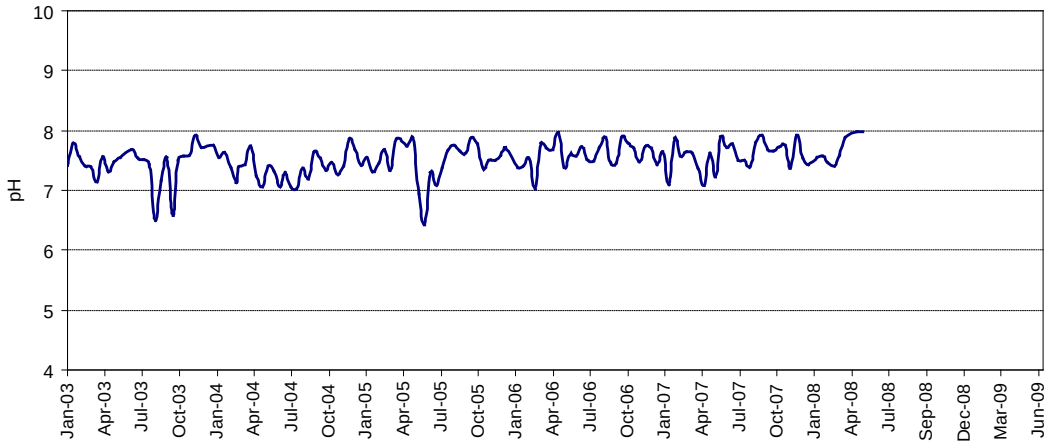

Figure 7.3 pH at Misverstand (Die Brug - G1H031Q01) from 1990 - 2008

Seasonal variation in pH within the estuary are presented in Figure 7.4 based on quarterly measurements collected during the period 2002 to 2005 (Schumann, 2007).

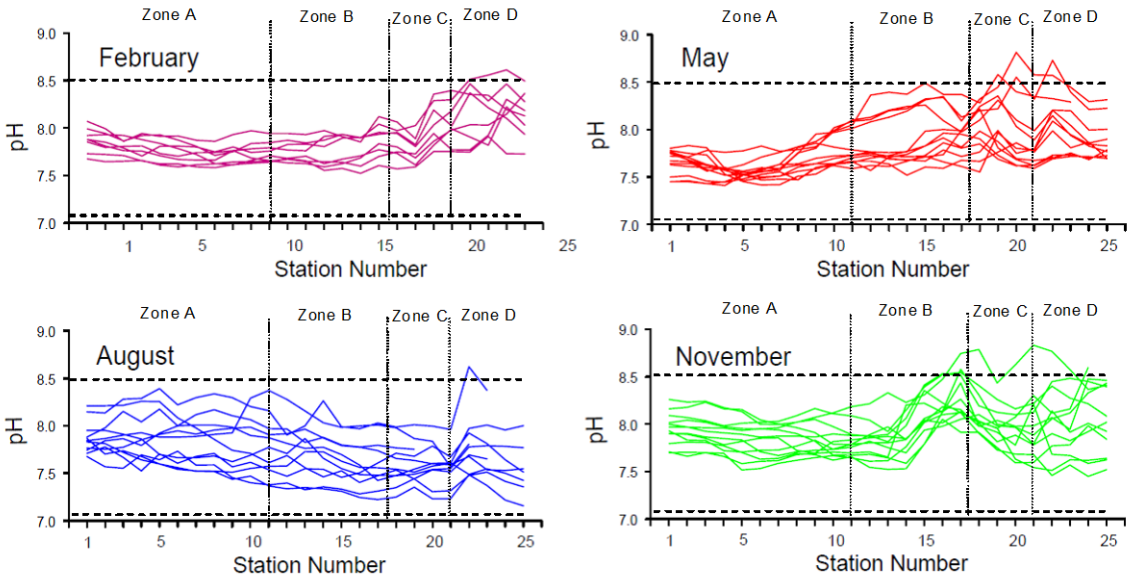

Figure 7.4 Vertically-integrated pH distribution in the Great Berg Estuary from 2003 -2005 (Schumann, 2007). Also indicated on the graphs are the different abiotic zone (Figure 5.1) and the 7 – 8.5 range (dotted lines)

Using the above information, typical pH distribution for all states are as follows:

Although the data show variability over the different seasons, pH levels in the estuary generally range between 7 and 8.5, applicable to all five abiotic states. Within this range the variability in pH is highest near the head of the estuary, reflecting the variability in the pH of river inflow (referring to Figure 7.3).

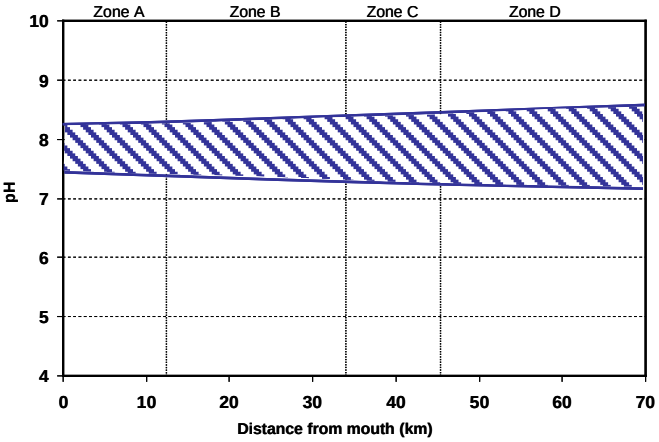

7.4 Dissolved Oxygen (DO)

Quarterly samples collected from BRM6 during 2003 and 2005 showed that the river water at this point (considered to be representative of river inflow to the estuary) was generally oxygenated averaging 10 mg/l during the colder winter months and 8 mg/l during the warmer summer period (Day, 2007). This is expected as DO concentrations are dependent on the prevailing salinity and temperature regimes. Under saturated or near-saturated conditions, dissolved oxygen concentrations are higher in fresher and/or colder waters compared with saline and/or warmer waters.

Seasonal variation in DO concentrations measured in the estuary are presented in Figure 7.5 based on quarterly measurements collected during the period 2002 to 2005 (Schumann, 2007).

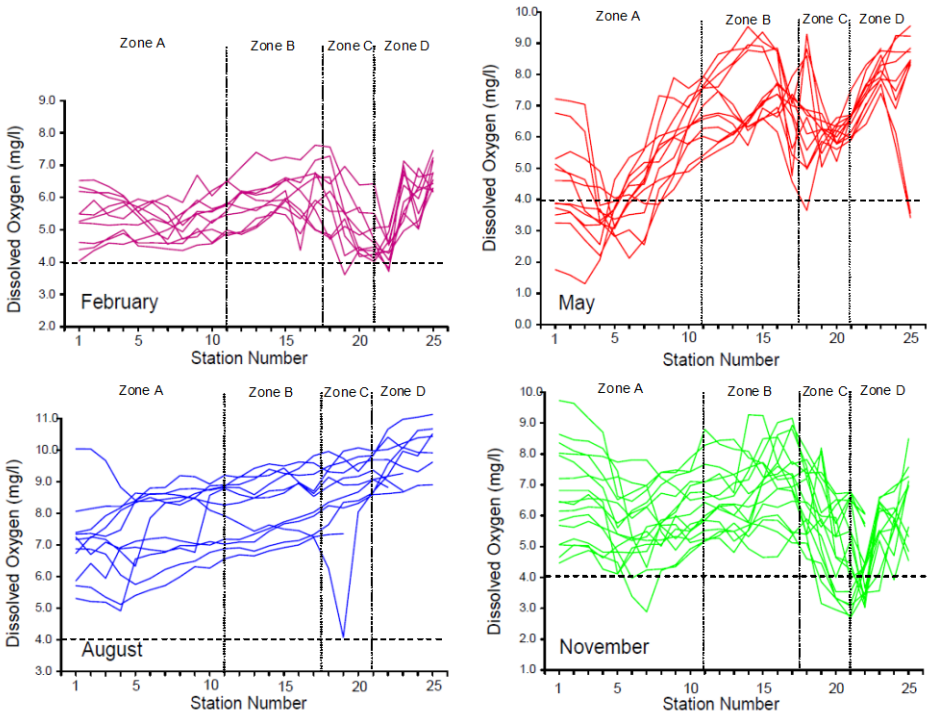

Figure 7.5 Vertically-integrated Dissolved oxygen distribution in the Great Berg Estuary from 2003 to 2005 (Schumann, 2007). Also indicated on the graphs are the different abiotic zone (Figure 5.1) and the 4 mg/l concentration (dotted lines)

The dependence of DO concentrations on temperature and salinity is apparent in Figure 7.5, i.e. colder and lower salinity waters have a higher saturation limit than warmer, saltier waters (Schumann, 2007).

Low DO concentrations measured on occasion near the mouth were associated with seawater intrusion from St Helena Bay that was identified as a zone for the formation of oxygen-deficient waters (Chapman and Shannon, 1985). A region within Zones C where lower DO concentrations was observed during the warmer months (e.g. Nov) was attributed to extensive organic loading from rotting vegetation (branches, leaves etc) and shading from riparian vegetation that inhibited photosynthesis (associated with exotic riparian vegetation – blue gums) (Clark and Taljaard, 2007).

Using the above information, typical DO distributions for the five abiotic states are as follows:

State 1: Severe marine dominated, State 2: Marine dominated

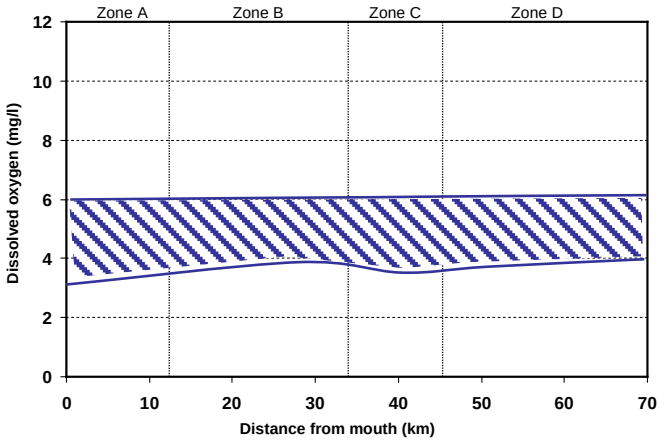

Oxygen in the system is generally > 4 mg/l but warmer temperature and long residence time is likely to keep levels below 6 mg/l. Low DO concentrations (<4 mg/l) may occur in Zone A on occasion as a result of oxygen deficient water being introduced from St Helena Bay. DO concentrations in a section of Zone C may also be lower at times as a result of high organic loading and inhibition of photosynthesis (associated with exotic riparian vegetation – blue gums) and long residence time.

State 3: Small to Medium Freshwater inflow

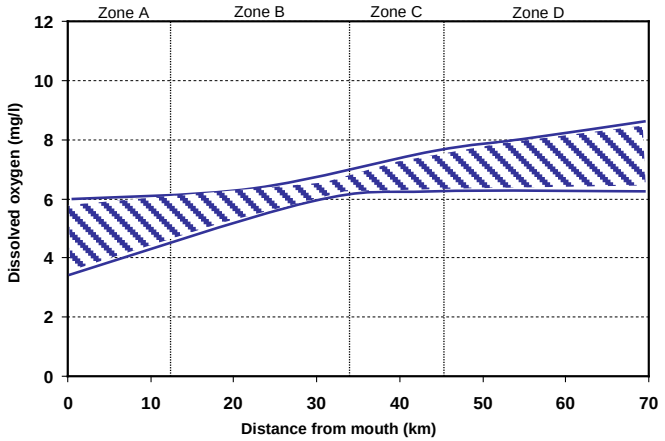

Oxygen in the system is generally ~6 mg/l although lower concentrations (<4 mg/l) may occur in Zone A on occasion as a result of oxygen deficient water being introduced from St Helena Bay. Improved freshwater flushing in the upper reaches elevates DO to >6 mg/l in Zones C and D.

State 4: Medium to high freshwater inflow & State 5: Freshwater dominated

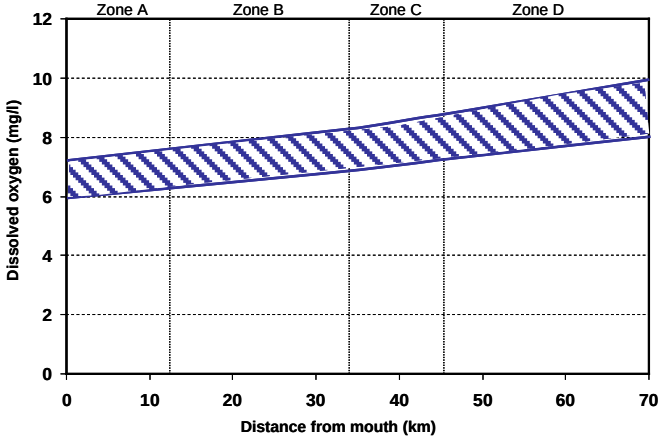

The system is well-oxygenated throughout (> 6 mg/l) as a result of strong freshwater flushing.

7.5 Secchi Depth (Transparency)

Only limited data on total suspended solids (TSS) is available on the lower Berg River (BRM6). TSS concentrations measured during quarterly sampling from 2003 to 2005 was ~20 mg/l, except on one occasion during autumn when the concentration was ~650 mg/l (Day, 2007). This high value could not be explained and did not coincide with any sudden increase in river flow.

Seasonal variation in Secchi depths measured in the estuary are presented in Figure 7.6 based on measurements collected during the period 2002 to 2005 (Schumann, 2007).

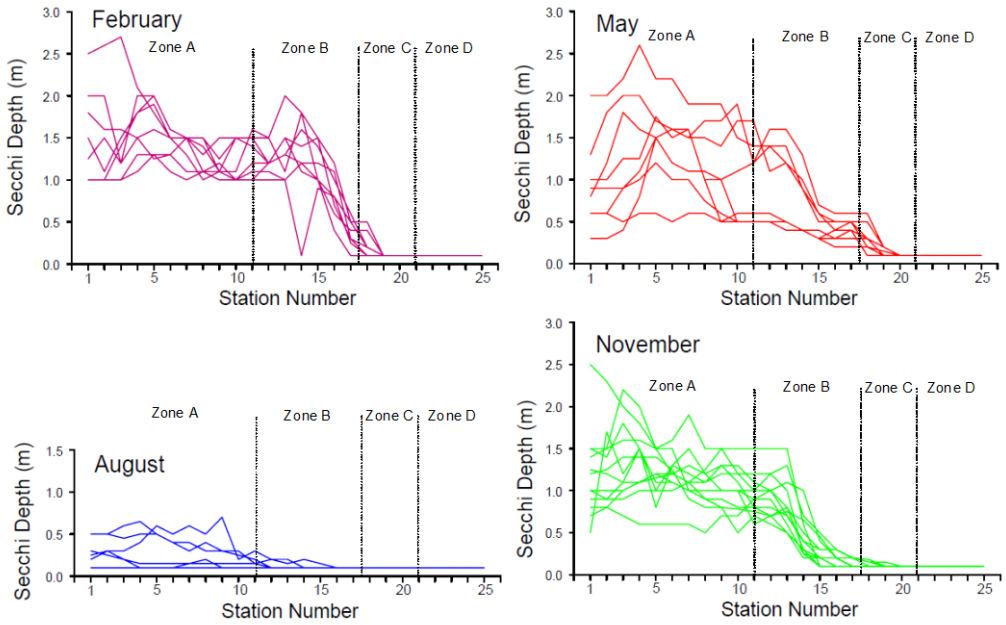

Figure 7.6 Secchi depths measured in the Great Berg Estuary from 2003 to 2005 (Schumann, 2007). Also indicated on the graphs are the different abiotic zone (Figure 5.1) and the 4 mg/l concentration line (dotted lines)

Secchi depths show a correlation with salinity distribution in that the highest turbidity (lowest Secchi depths) is measured at the freshwater front and further upstream, indicating that these high turbidity probably originate from river inflow. Schumann (2007) observed that the colour of the water in the estuary could classify as “murky” brown, while occasionally clearer seawater was present near the mouth.

Using the above information, typical Secchi depth distributions for the five abiotic states are as follows:

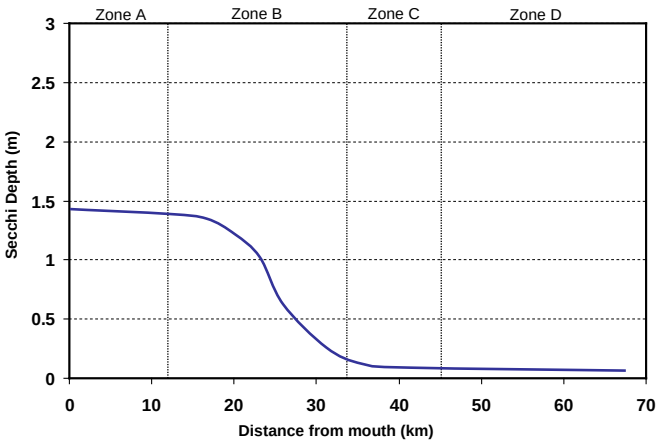

<u>State 1: Severe marine dominated</u>

During this state a strong seawater signal extends somewhat into Zone B, resulting in relatively high transparency (Secchi depth) downstream towards the mouth. A marked reduction in transparency occurs at the

freshwater front (~30 km from the mouth) with relatively low Secchi depths upstream of this region.

State 2: Marine dominated

During this state a strong seawater signal extends somewhat into Zone B, resulting in relatively high transparency (Secchi depth) downstream towards the mouth. A marked reduction in transparency occurs at the freshwater front (~25 km from the mouth) with relatively low Secchi depth upstream of this region.

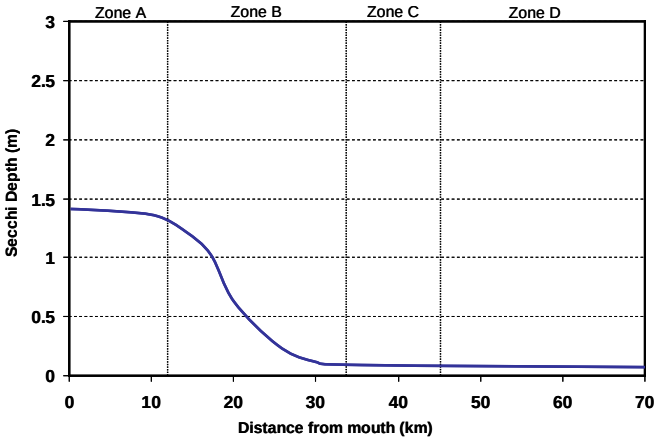

State 3: Small to Medium Freshwater inflow

During this state a strong seawater intrusion is limited to Zone A, resulting in relatively high transparency (Secchi depth) downstream towards the mouth. A marked reduction in transparency occurs at the freshwater front (~15 km from the mouth) with relatively low Secchi depth upstream of this region.

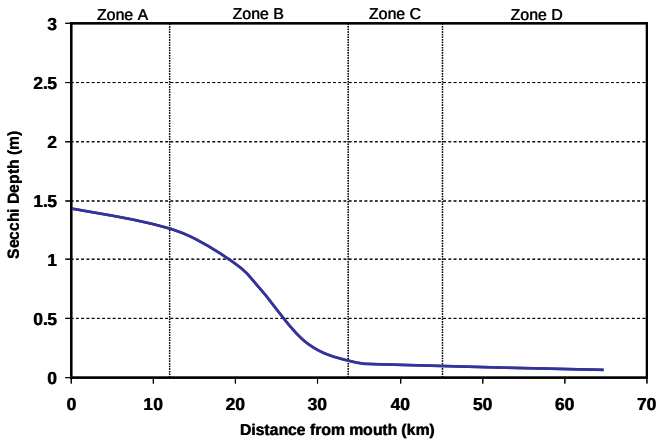

State 4: Medium to high freshwater inflow

During this state only some seawater intrusion are evident in Zone A (slightly higher transparency), but strong river influence results in low transparency (Secchi depths) throughout Zones B-C.

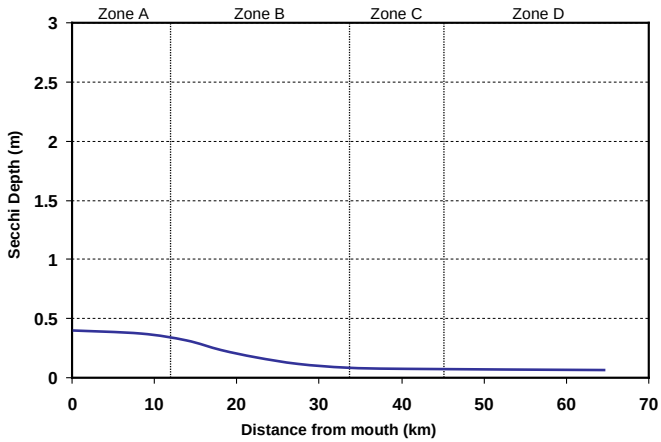

State 5: Freshwater-dominated

Strong river inflow results in low transparency (Secchi depths) throughout the system.

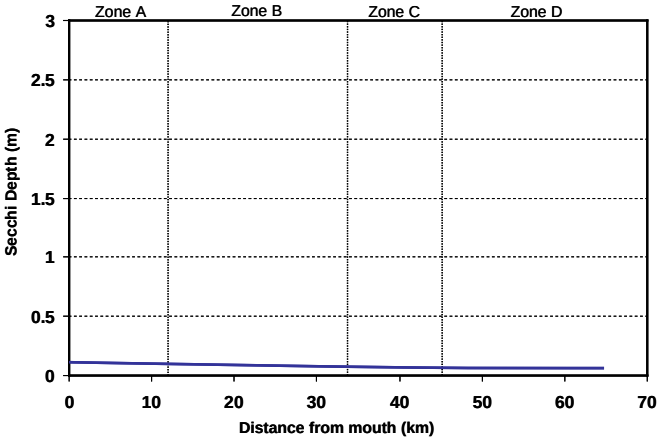

7.6 Dissolved Inorganic Nitrogen (DIN)

DIN (NO_x-N + NH_4-N) concentrations in river inflow, considered to be representative of the Present State are represented in Figure 7.7 (in the Berg River, DIN mainly comprise NO_x-N).

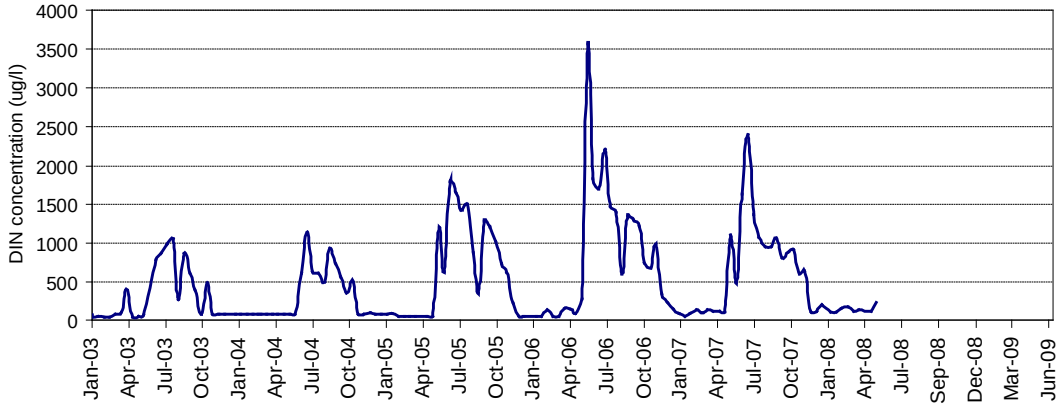

Figure 7.7 DIN concentrations at Misverstand (Die Brug - G1H031Q01) from 2003 – 2008 (representative of Present State)

Results show a very strong seasonal signal where DIN concentrations in the dry (summer) months drop are generally less than 100 µg/l to greater than 1000 µg/l in the wetter months associated with agricultural activities (fertilizer use) in the catchment). Autumn/winter maxima appear to be linked to increased flow in the river channel (Day, 2007): DIN decreased sharply as flow increased towards a flood peak, but as flood peak declined, DIN concentrations increased sharply, mirroring to some extent the shape of the flood peak. There are no DIN records for the Berg River in an unimpacted state (reference condition). Considering lower Berg River (Kersefontein) data of 1950s, summer concentrations were low (<100 µg/l), while concentrations in winter (wet season) averaged 400 µg/l, much lower than the winter peaks of the Present State (Day, 2007). Based on the catchment geology it can be expected that even under the reference condition nutrient concentrations in the lower reaches of the river would have been higher compared with the acidic, low-nutrient character of the upper reaches. However, in the 1950s agriculture in the catchment was already extensive and it is therefore assumed that DIN concentrations in the lower river most likely have been even lower than in the 1950s, ~100 µg/l or less.

DIN input (mainly as NO_3-N) to the Berg Estuary from the sea occurs during upwelling events mostly in summer (Slinger and Taljaard 1994). The prevailing south-easterly winds at this time of the year drive surface water offshore allowing nutrient rich waters to well-up from below along the coast (Chapman and Shannon 1985). Tidal processes transport these into the Berg Estuary contributing to nutrient supply particularly in the lower estuary. Corresponding northerly winds that prevail in winter (the high flow season) tend to drive nutrient poor surface waters onshore which in turn provide a very modest contribution to nutrient supplies to the estuary. Typical DIN concentrations for newly upwelled water and oceanic surface water in the Benguela region are 200-400 µg/l and 110-140 µg/l, respectively (Chapman and Shannon1985, Bailey and Chapman 1991).

The inorganic nutrient concentrations in an estuary are largely a function of the concentrations in the source waters, i.e. the river and the sea, as well as any physical (e.g. evaporation),

geochemical (e.g. adsorption/desorption and flocculation) and/or biochemical processes (e.g. biological uptake and re-mineralisation) that occur within the estuary. The extent to which these processes affect inorganic nutrient characteristics in the Great Berg Estuary is discussed below. An approach that is widely used to assess nutrient cycling and transformation in estuaries is the use of mixing diagrams (or property-salinity plots) (e.g. Ferguson et al., 2004; Eyre, 2000; Eyre & Balls, 1999). The mixing diagram approach consists of a plot of nutrient concentrations against salinity along the estuarine gradient. This provides a convenient method for visualising the net effect of nutrient processes within estuaries whereby deviation from the conservative mixing line is used to interpret results. For example, downward curvature in the mixing diagram implies nutrient uptake, while upward curvature implies nutrient release. To orientate oneself in terms of the spatial distribution of nutrient concentrations along the estuary, the nutrient versus salinity plots should be compared with corresponding longitudinal salinity profiles provided in Chapter 7.2. The mixing diagrams for inorganic nitrogen measurements in the Great Berg Estuary are presented in Figure 7.8.

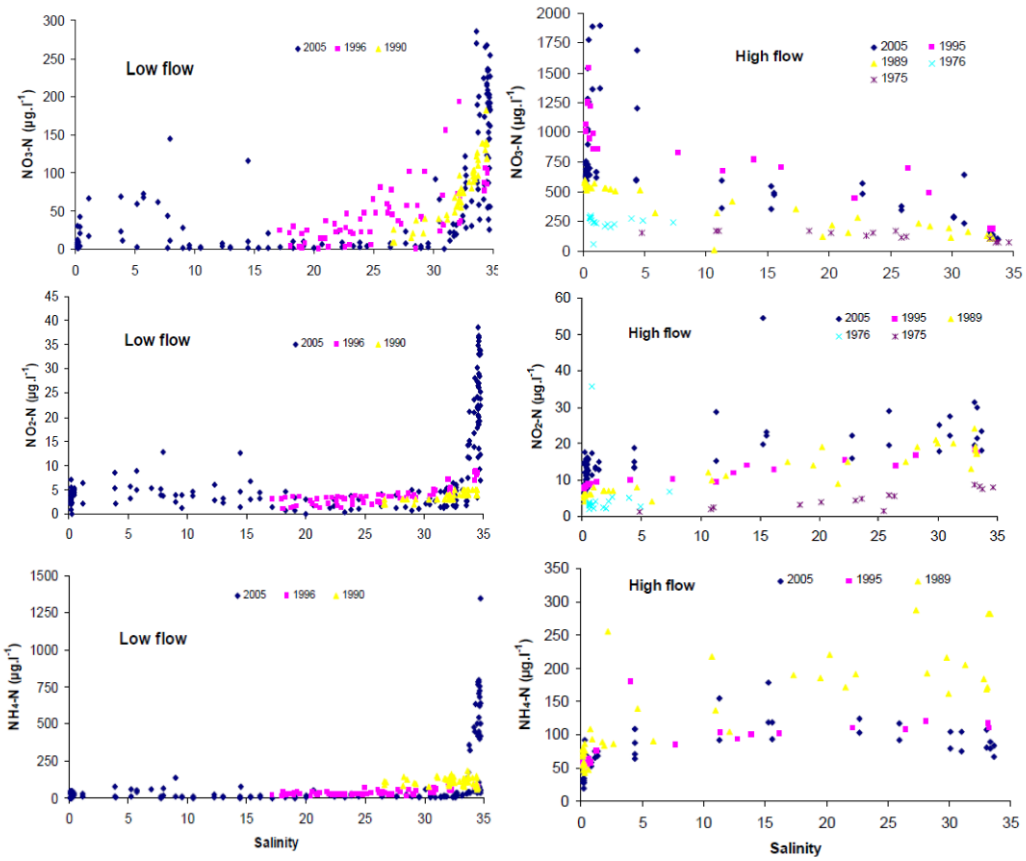

Figure 7.8 Inorganic nitrogen concentrations measured in the Berg River Estuary during low and high flow periods from 1975 – 2005 (exceptionally high NH4-N concentrations during "Low flow" were limited to the May 2005 survey, probably linked to significant anthropogenic inputs at the time) (Clark and Taljaard, 2007)

DIN concentrations in the estuary show strong seasonal patterns. During summer when river inflow is low, DIN concentrations throughout the estuary is generally low (<100 µg/l), except at high

salinities (~35), where DIN concentrations at times reached ~500 µg/l. Upwelling is most likely the primary source of DIN (mainly as NO_3-N) during these periods, while anthropogenic sources (e.g. fish factory effluent and ballast discharges from fishing vessels) are probably also contribute (mainly as NH_4-N).

During winter, when river inflow is high, it becomes the major source of DIN to the estuary with concentrations typically exceeding 1000 µg/ in the fresher parts of the estuary. Relatively low DIN concentrations at high salinities (~35) indicate that upwelling is not a major source of DIN during the winter months.

NOTE:

Differences in the rates of uptake of different inorganic nutrients (N, P and Si) suggests that N is most limiting in the Great Berg Estuary, as is generally the case in the marine environment (Chapman and Shannon 1985). While it is difficult to prove conclusively that nitrogen is indeed limiting in this estuary without accurately measuring rates of algal growth under variable nutrient concentrations, comparing nutrient concentrations in the environment with known half saturation constants (i.e. the concentration at which nutrient uptake is half its maximum value) does provide a good indication of whether this is the case or not (Fisher et al. 1988). Below this value, uptake rates are reduced potentially to the extent that they limit algal growth rates or biomass accumulation, while above this level nutrient concentration is likely to have a small positive effect on uptake rates (Fisher et al. 1988). Half saturation constants reported in the literature for DIN in the order of (14-28 µg/l) (MacIsaac and Dugdale 1969, Eppley et al. 1969, Murphy 1980, Fisher et al. 1981, Priscu and Priscu 1984), DIP in the order 3-15 µg/l (Nalewajko and Lean 1980) and DRS in the order of 28-140 µg/l) (Paasche 1973).

Nutrient concentrations in the Great Berg (Figure 7.7) suggests that DIN reaches concentrations that are potentially limiting particularly in the mid-salinity ranges during low flows (dry season), while DIP is at potentially limiting levels only in the extreme upper reaches of the estuary during these periods. DRS most likely never reach concentrations that are considered limiting (Clark and Taljaard, 2007).

Using the above information, typical DIN distributions for the five abiotic states are as follows:

State 1: Severe marine dominated

During this state Zone A and lower section of Zone B are subject to tidal flushing (salinity ~35) that introduce high DIN to this section (assuming state occurs in summer when upwelling is frequent), possibly also anthropogenic inputs form fishing activities taking place during summer. Further upstream DIN becomes largely depleted in the water column as a result of long residence time. During summer (dry season) the river is not a major source of DIN to the estuary.

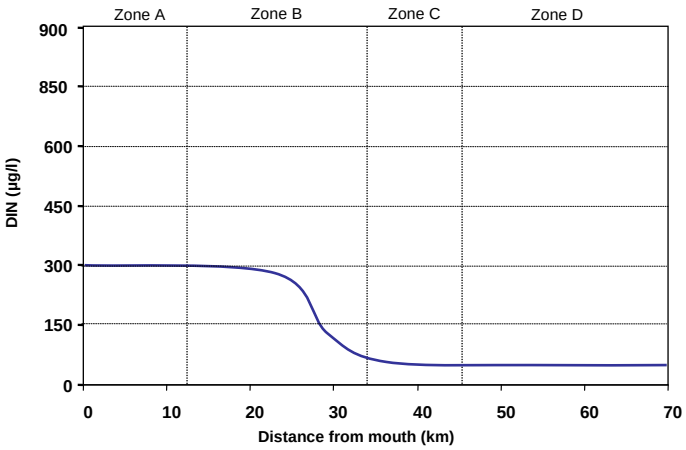

State 2: Marine dominated

During this state Zone A is subject to tidal flushing (salinity ~35) that introduces high DIN to this section (assuming state occurs in summer when upwelling is frequent), possibly also anthropogenic inputs form fishing activities taking place during summer. Further upstream DIN becomes largely depleted in the water column as a result of long residence time. During summer (dry season) the river is not a major source of DIN to the estuary.

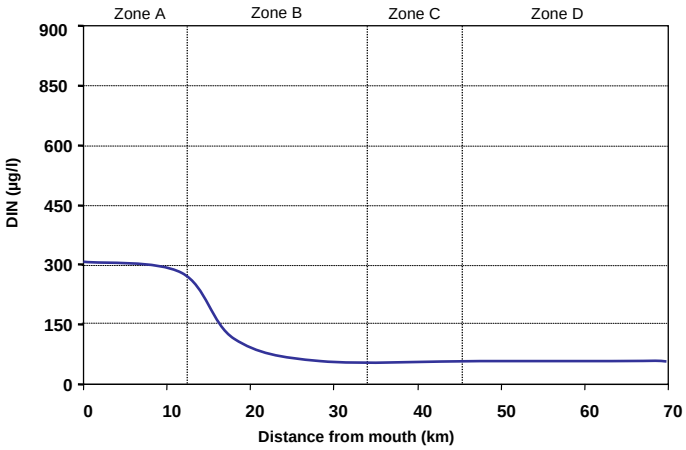

State 3: Small to Medium Freshwater inflow

During this state marine influence are limited to Zones A and B. Under the Present situation, this state would typically occur in autumn/spring when upwelling is less frequent and the sea no longer a major source of DIN to the estuary. With stronger freshwater inflow (and relatively higher DIN concentrations associated with anthropogenic inputs), the river is now a major source of DIN particularly in Zones C and D. Limited flushing in Zone B, accounts for some removal of DIN. Note, under the reference condition this state was probably typical of summer. As a result, the sea (through upwelling), would have been a major source of DIN in Sections A and B, while DIN in Sections C and D would have been much lower compared with the Present (i.e. no anthropogenic inputs).

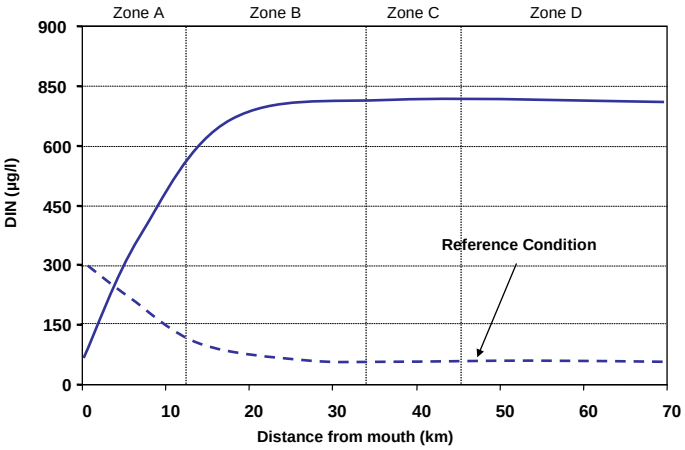

State 4: Medium to high freshwater inflow

During this state marine influence are limited to Zones A. Assuming this state would typically occur during the wet season (winter) when upwelling is less frequent and the sea no longer a major source of DIN to the estuary. Under the Present situation, with strong freshwater inflow (and high DIN concentrations associated with anthropogenic inputs), the river is now a major source of DIN particularly in Zones B-D. Note, under the reference condition, DIN would have been much lower throughout the estuary compared with the Present (i.e. no anthropogenic inputs in river inflow).

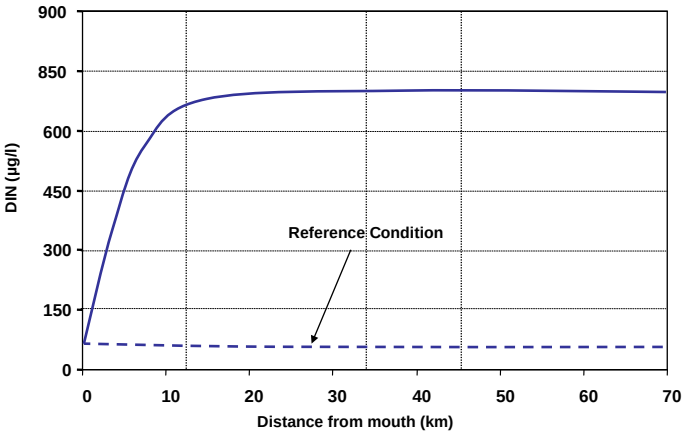

State 5: Freshwater-dominated

During this state DIN concentration in the estuary is dictated by concentrations in river inflow, which under the Present Situation in high. Saline intrusion into Zone A introduces low DIN concentrations into the lower reaches during spring high tides. Note, under the reference condition, DIN would have been much lower throughout the estuary compared with the Present (i.e. no anthropogenic inputs in river inflow).

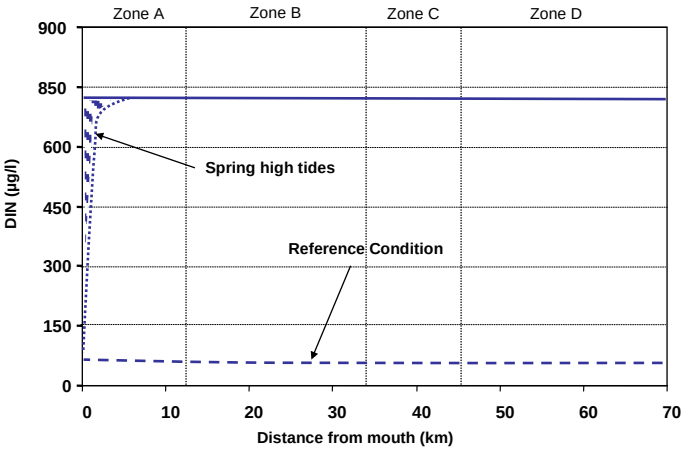

7.6 Dissolved Inorganic Phosphate (DIP)

DIP concentrations in river inflow, considered to be representative of the Present State, are represented in Figure 7.9.

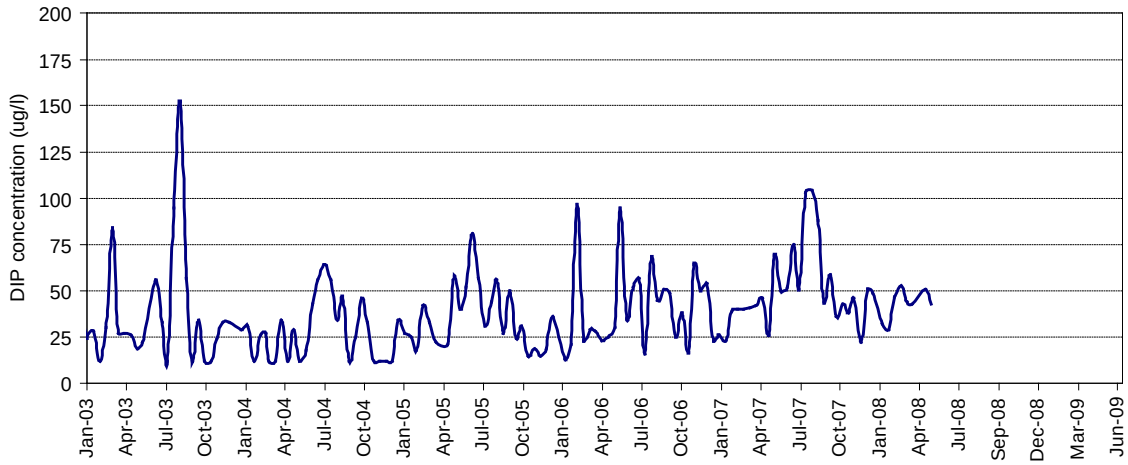

Figure 7.9 DIP concentrations at Misverstand (Die Brug - G1H031Q01) from 2003 – 2008 (representative of Present State)

Results do not show any clear seasonal signal, but there is a tendency for summer concentrations to be lower (< 50 µg/l) compared with winter periods (winter concentrations show high variability, but seldom exceed 100 µg/l). These relatively low DIP concentrations are surprising considering the extensive anthropogenic inputs (e.g. agricultural activities and wastewater) but could be linked to P being strongly associated with soils compared with inorganic N that are very mobile (Clark and Taljaard, 2007). There are no DIP records for the Berg River in an unimpacted state (reference condition). However, lower Berg River (Kersefontein) data of the 1960s, showed low concentrations during both summer and winter (< 30 µg/l) (Day, 2007). This suggests that under the reference condition (when agricultural activities were less) DIP concentrations would at least have been < 30 µg/l (possibly lower).

Similar to DIN, DIP input to the Great Berg Estuary from the sea occurs during upwelling events mostly in summer (Slinger and Taljaard 1994). Typical DIP concentrations for newly upwelled water and oceanic surface water in the Benguela region are 40-90 µg/l and 50-56 µg/l, respectively

(Chapman and Shannon1985; Bailey and Chapman 1991). The mixing diagrams for DIP measurements in the Great Berg Estuary are presented in Figure 7.10.

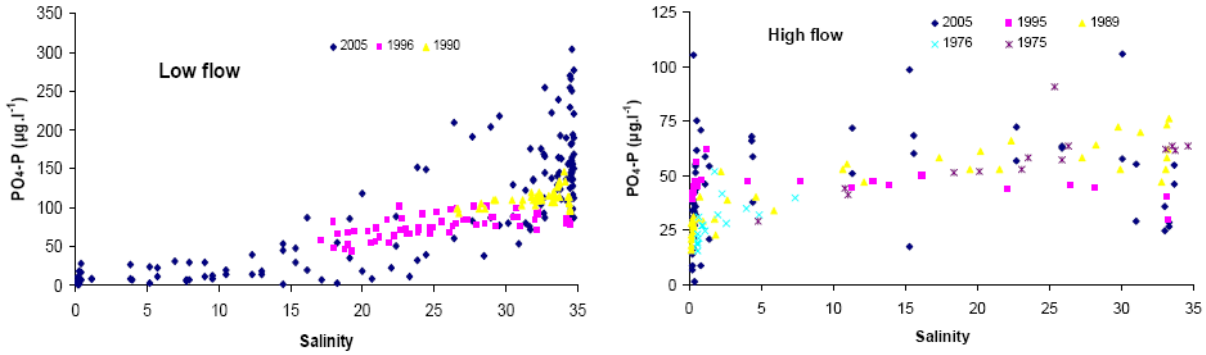

Figure 7.10 DIP concentrations measured in the Berg River Estuary during low and high low periods from 1975 – 2005 (Clark and Taljaard, 2007)

During low flows (summer) low DIP concentrations in the fresher parts (<50 µg/l) of the estuary were similar to that in measured in river inflow during summer (Figure 7.9). High DIP concentrations measured in more the saline waters (~35) during low flows show the influence of upwelling, frequently occurring in summer along this part of the coast. However, DIP concentrations in saline waters often exceeded concentrations expected for recent upwelled waters (> 90 µg/l). Anthropogenic input from (e.g. fisheries and waste disposal along the banks) was considered as likely sources (Clark and Taljaard, 2007). During high flow periods (winter) DIP concentrations throughout the estuary was relatively low. This was expected since upwelling is less frequent during winter and DIP concentrations in river inflow remain relatively low even during high flows (although more variable compared with low flow periods).

Using the above information, typical DIP distributions for the five abiotic states are as follows:

State 1: Severe marine dominated

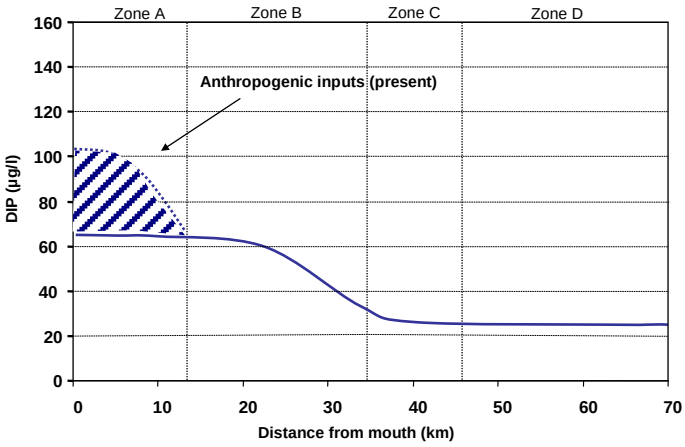

During this state Zone A and lower section of Zone B are subject to tidal flushing (salinity ~35) that introduce higher DIP to this section (assuming state occurs in summer when upwelling is frequent). Anthropogenic inputs in Zone A (fishing activities taking place during summer) also contribute significantly. Further upstream DIP decreased linked to low DIP concentrations in river inflow and in situ uptake (longer residence times). During the reference conditions inputs from the river would have been slightly lower compared with the present

State 2: Marine dominated

During this state Zone A is subject to tidal flushing (salinity ~35) that introduces high DI to this section (assuming state occurs in summer when upwelling is frequent). Anthropogenic inputs in Zone A (fishing activities taking place during summer) also contribute significantly. Further upstream DIP decreased linked to low DIP concentrations in river inflow and in situ uptake (longer residence times). During the reference conditions inputs from the river would have been slightly lower compared with the present.

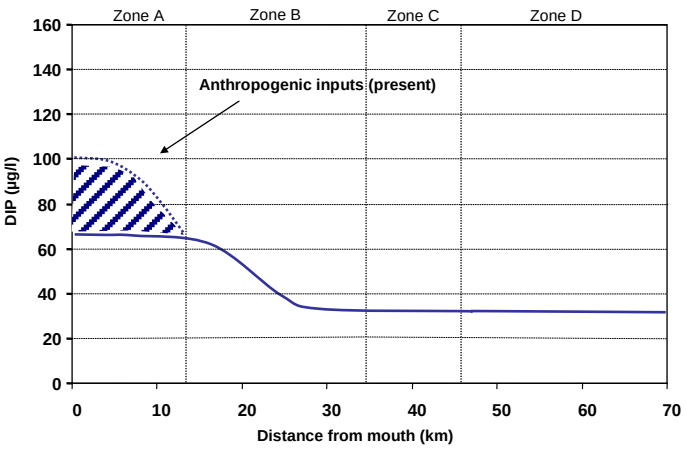

State 3: Small to Medium Freshwater inflow

During this state marine influence are limited to Zones A and B. Under the Present situation, this state would typically occur in autumn/spring when upwelling is less frequent and the sea no longer a major source of DIP to the estuary. Further upstream DIP increase to some extent as higher river flows introduce elevated concentrations. Note, under the reference condition this state was probably typical of summer. As a result, the sea (through upwelling), would have been a major source of DIN in Sections A and B, while DIP in Sections C and D would have been much lower compared with the Present (i.e. no anthropogenic inputs).

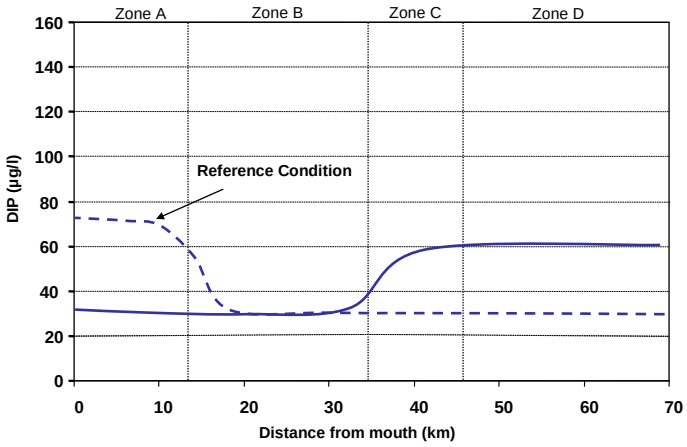

State 4: Medium to high freshwater inflow

During this state (typical of winter) upwelling is less frequent and the sea no longer a source of DIP to the estuary. Under the Present situation, DIP concentrations in the estuary are relatively low, but elevated compared with reference condition (i.e. as a result of anthropogenic inputs), except in Zone A where limited seawater intrusion is still evident

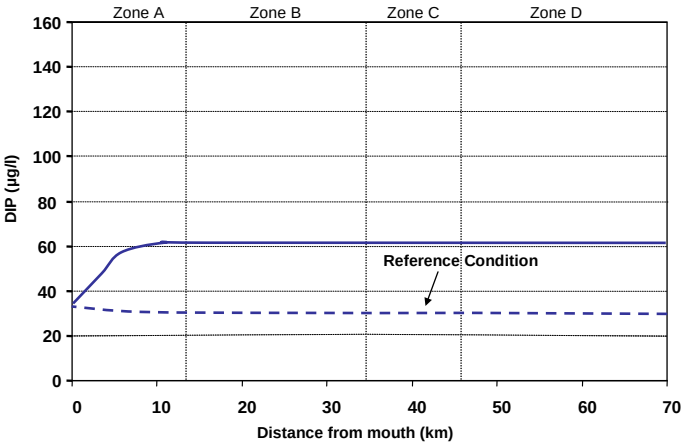

State 5: Freshwater-dominated

During this state (typical of winter) upwelling is less frequent and the sea no longer a source of DIP to the estuary. Under the Present situation, DIP concentrations in the estuary are relatively low, but elevated compared with reference condition (i.e. no anthropogenic inputs in river inflow).

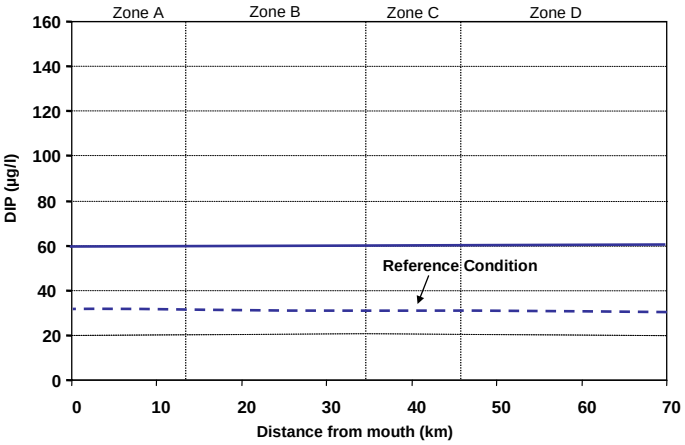

7.7 Dissolved reactive Silicate (DRS)

DRS concentrations in river inflow, considered to be representative of the Present State, are represented in Figure 7.11.

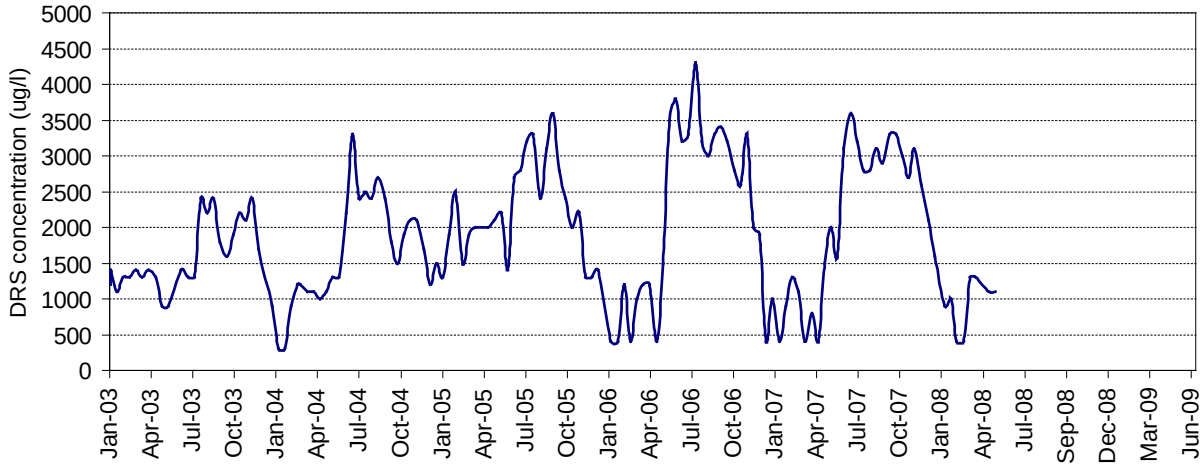

Figure 7.11 DRS concentrations at Misverstand (Die Brug - G1H031Q01) from 2003 – 2008 (representative of Present State)

The data, particularly since 2006, show a distinct seasonal pattern where DRS concentrations during average DRS concentrations in summer is low (<1000 µg/l) increasing to concentrations >3000 µg/l during winter. There are no DRS records for the Berg River in an unimpacted state (reference condition). Considering the temporal increase suggested in DRS measurements in freshwater parts of the estuary during high flows (Figure 7.11), natural concentrations in river inflow may have been somewhat lower than at present (e.g. as a result of land-use and increased erosion under the present state). However, DRS is naturally high in river water, compared with seawater, linked to catchment geological characteristics. Assume therefore the reference condition as ~2000 µg/l.

Significant DRS input to the Great Berg Estuary from the sea occurs during upwelling events mostly in summer (Slinger and Taljaard 1994). Typical DRS concentrations for newly upwelled water and oceanic surface water in the Benguela region are 140-1400 µg/l and 330-360 µg/l, respectively (Chapman and Shannon1985; Bailey and Chapman 1991).

The mixing diagrams for DRS measurements in the Great Berg Estuary are presented in Figure 7.12.

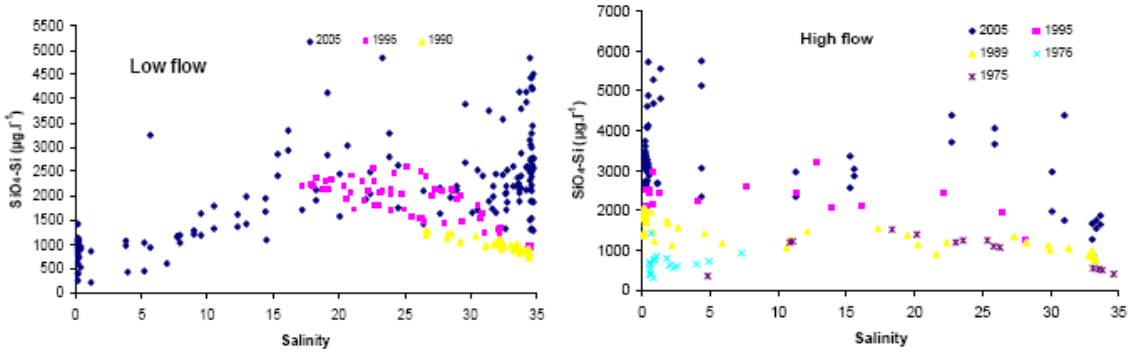

Figure 7.12 DRS concentrations measured in the Berg River Estuary during low and high flow periods from 1975 – 2005 (Clark and Taljaard, 2007)

Considering the concentrations of DRS in sea- and river water (Figure 7.10) it is expected for DRS concentrations to increase with a decrease in salinity. This trend was evident in the high flow period and in the historical data for the low flow period, but not during the 2005 surveys. This was surprising as in most systems (including historical data for the Great Berg) the reverse relationship is expected (Eagle and Bartlett, 1984).

Using the above information, typical DRS distributions for the five abiotic states are as follows:

<u>State 1: Severe marine dominated</u>

During this state Zone A and lower section of Zone B are subject to tidal flushing (salinity ~35) that introduce lower DRS to these zones estuary. Further upstream DRS concentrations are elevated, influenced by river inflow.

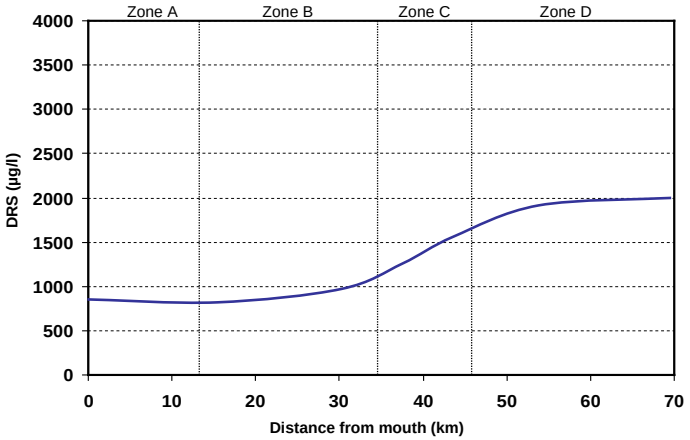

<u>State 2: Marine dominated</u>

During this state Zone A is subject to tidal flushing (salinity ~35) that introduce lower DRS to the estuary. Further upstream DRS concentrations are elevated, influenced by river inflow.

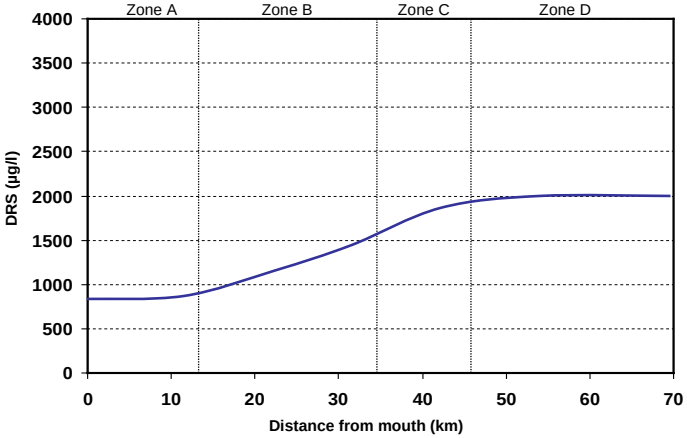

State 3: Small to Medium Freshwater inflow

During this state strong marine influence are limited to Zones A. Elevated DRS in river inflow is evident upstream, particularly in Section C and D.

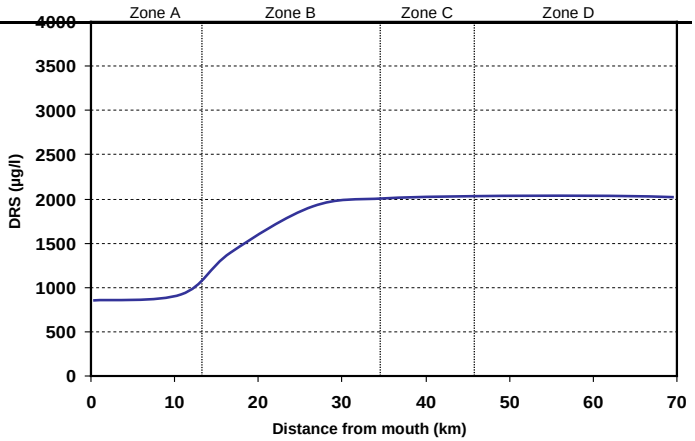

State 4: Medium to high freshwater inflow

During this state (winter) marine influence are limited to Zones A. Significantly elevated DRS in river inflow is evident, particularly in Section B-D. DRS in river inflow are elevated under the Present state compared to Reference conditions, possibly linked to increase erosion in catchment.

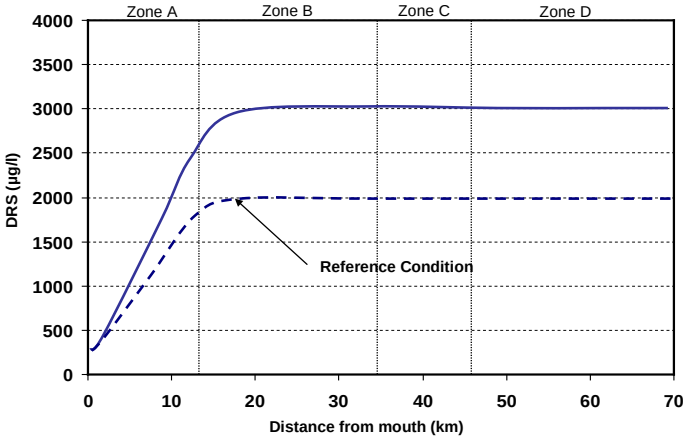

State 5: Freshwater-dominated

During this state (winter) marine influence are limited to lower section of Zones A only during spring high tides. Significantly elevated DRS in river inflow is evident throughout the estuary. DRS in river inflow are elevated under the Present state compared to Reference conditions, possibly linked to increase erosion in catchment.

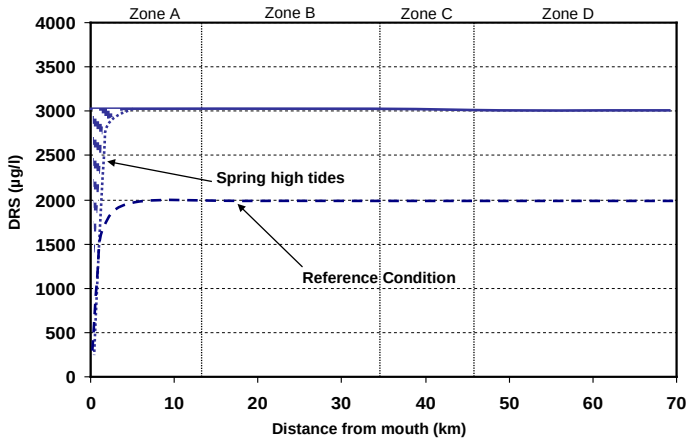

Table 0.1 Summary of typical hydrodynamic and water quality characteristics of different abiotic states in the Great Berg Estuary

PARAMETER	STATE 1	STATE 2	STATE 3	STATE 4	STATE 5
River flow (m^3/s)	**0.5**	0.5-1	**1-5**	**5-25**	**>25**
Mouth condition	**Open**	**Open**	**Open**	**Open**	**Open**
Inundation	No Inundation of floodplain	No Inundation of floodplain	No Inundation of floodplain	No Inundation of floodplain	**Extensive** inundation of floodplain
Salinity (ppt)	**35 / 33-20 / 20-5 / 5**	**33 / 30-10 / 10-5 / <5**	Present: **33-25 / 25-5 / <5 / <5**; or **33-20 / 20-5 / <5 / <5**; Reference	**33-5 / <5 / <5 / <5**	**<5 / <5 / <5 / <5**
Temperature (°C)	**12-20 / 20-25 / 26 / 26**		**13-20 / 20-25 / 24 / 24**	**12-18 / 12-18 / 12-18 / 12-18**	
pH	**7.5-8.3 / 7.5-8.3 / 7-8.5 / 7-8.5**				
DO (mg/l)	**4-6 / 4-6 / 4-6 / 4-6**		**4-6 / 4-6 / >6 / >6**	**>6 / >6 / >6 / >6**	
Transparency (Sechhi depth in m)	**>1.2 / ~0.7 / <0.2 / <0.2**			**~0.7 / <0.2 / <0.2 / <0.2**	**<0.2 / <0.2 / <0.2 / <0.2**
DIN (µg/l)	**~300 / ~300 / <80 / <80**	**~300 / <80 / <80 / <80**	Present: **<80 / ~300 / >800 / >800**; or **~300 / <80 / <80 / <80**; Reference	Present: **300 / >800 / >800 / >800**; or **<80 / <80 / <80 / <80**; Reference	Present: **>800 / >800 / >800 / >800**; or **<80 / <80 / <80 / <80**; Reference
DIP (µg/l)	Present: **>100 / ~60 / <30 / <30**; or **~60 / ~60 / <30 / <30**; Reference	Present: **>100 / <30 / <30 / <30**; or **~60 / <30 / <30 / <30**; Reference	Present: **<30 / <30 / <30 / ~60**; or **~60 / <30 / <30 / <30**; Reference	Present: **<30 / ~60 / ~60 / ~60**; or **<30 / <30 / <30 / <30**; Reference	Present: **~60 / ~60 / ~60 / ~60**; or **<30 / <30 / <30 / <30**; Reference
DRS (µg/l)	**<1000 / <1000 / <1000 / ~2000**		**<1000 / <1000 / ~2000 / ~2000**	Present: **<1000 / >3000 / >3000 / >3000**; or **<1000 / ~2000 / ~2000 / ~2000**; Reference	Present: **>3000 / >3000 / >3000 / >3000**; or **~2000 / ~2000 / ~2000 / ~2000**; Reference

NOTE: For the purposes of this assessment the estuary was sub-divided into 4 zones representing from left to right: Zone A (0-12 km), Zone B (12-33 km), Zone C (33-45 km) and Zone D (45-70 km)

8 References

Bailey, G.W. and Chapman, P. (1991) Short-term variability during an anchor station study in the southern Benguela upwelling system: Chemical and physical oceanography. *Progress in Oceanography,* 28(1-2): 9-37.

Chapman, P. and Shannon, L.V. (1985) The Benguela ecosystem Part ll. Chemistry and related processes. Oceanogr. *Mar. Biol. Ann. Rev*., 23: 183-251.

Clark, B.M. and Taljaard, S (2007) Chapter 4 – Water Chemistry: Nutrients. In: Berg River Baseline Monitoring Programme Final Report - Volume 3: Estuary And Floodplain Environment. Clark, B.M. & Ratcliffe G. (Eds). Report prepared for the Department of Water Affairs and Forestry, DWAF Report No. P WMA 19/G10/00/1907. Pretoria.

Day, J. (Ed.) (1981). Estuarine ecology with particular reference to Southern Africa. Cape Town. A.A. Balkema. 411 pp.

Day, L (2007) Chapter 4 – Water Chemistry. In: Berg River Baseline Monitoring Programme Final Report - Volume 3: Riverine Baseline Monitoring Programme and Statement of Baseline Conditions. Ratcliffe (Ed.). Report prepared for the Department of Water Affairs and Forestry, DWAF Report No. P WMA 19/G10/00/1807. Pretoria

De Cuevas, B.A., G.B. Brundrit and A.M. Shipley (1986) Low-frquency sea-level fluctuations along the coasts of Namibia and South Africa, *Geophysical Journal of the Royal Astronomical Society*, 87: 33-42.

Department of Water Affairs and Forestry (DWAF) (2007) Berg River Baseline Monitoring Programme Final Report - Volume 3: Estuary And Floodplain Environment. Clark, B.M & Ratcliffe G. (Eds). Report prepared for the Department of Water Affairs and Forestry, DWAF Report No. P WMA 19/G10/00/1907. Pretoria.

Department of Water Affairs and Forestry (DWAF) (2008) Water Resource Protection and Assessment Policy Implementation Process. Resource Directed Measures for protection of water resources: Methodology for the Determination of the Ecological Water Requirements for Estuaries. Version 2. Pretoria.

Duvenhage, I.R. (1983) Getyrivier opervlakktes van sommige getyriviere aan die Kaapse kus. Report produced by ECRU (unpublished). CSIR, Stellenbosch.

Eagle, G.A and Bartlett, P.D. (1984) Preliminary chemical studies in four Cape estuaries. CSIR Report T/SEA 8307. CSIR, Stellenbosch.

Eyre, B. (2000) Regional evaluation nutrient transformation and phytoplankton growth in nine river dominated sub-tropical east Australian estuaries. *Marine Ecology Progress Series,* 205: 61-83.

Eyre, B. and Ball, P.W. (1999) A comparative study of nutrient behaviour along the salinity gradient of tropical and temperate estuaries. *Estuaries*, 22 (2A): 313-326.

Ferguson, A., Eyre, B. and J. Ga (2004) Nutrient cycling in the sub-tropical Brunswick Estuary, Australia. *Estuaries*, 27 (1): 1-17.

Fisher T.R., Carlson. P.R. and Barber, R.T. (1981) Some problems in the interpretation of ammonium uptake kinetics. *Marine Biology Letters,* 2: 33-44.

Fisher T.R., Harding L.W., Stanley D.W. and Ward, L .G. (1988) Phytoplankton, nutrients and turbidity in the Chesapeake, Delaware and Hudson estuaries. *Estuarine Coastal and Shelf Science*, 27: 61-93.

Hughes, P., G.B. Brundrit & F.A. Shillington (1991) South African sea-level measurements in the global context of sea-level rise. *South African Journal of Science*, 87: 447-453.

Huizinga, P., Slinger, J.H. and J. Boroto (1994) the hydrodynamics of the Berg River estuary – a preliminary evaluation with respect to mouth entrainment

MacIsaac, J.J. & R.C. Dugdale. (1969) The kinetics of nitrate and ammonium uptake by natural populations of marine phytoplankton. *Deep Sea Research*, 16: 343-346.

Murphy, T.P. (1980) Ammonia and nitrate uptake in the lower Great Lakes. *Canadian Journal of Fisheries and Aquatic Science,* 37: 1365-1372.

Nalewajko, C. and Lean, D.R.S. (1980) Phosphorus. In: Morris, I. (Ed.) The Physiological Ecology of Phytoplankton. Blackwell Scientific, Oxford, 00. 235-258.

Paasche, E. (1973) Silicon and the ecology of marine plankton diatoms. II: Silica uptake kinetics in five diatom species. *Marine Biology*, 19: 262-169.

Priscu, J.C. and Priscu, L R. (1984) Inorganic nitrogen uptake in oligotrophic Lake Taupo, New Zealand. Canadian Journal Fisheries Research Board, 41: 1436-1445.

Schumann, E. (2007) Chapter 3: Water Chemistry - Salinity, Temperature, Oxygen and Turbidity. *In:* Berg River Baseline Monitoring Programme Final Report - Volume 3: Estuary And Floodplain Environment. Clark, B.M & Ratcliffe G. (Eds). Report prepared for the Department of Water Affairs and Forestry, DWAF Report No. P WMA 19/G10/00/1907. Pretoria.

Shillington, F.A. (1984) Long period edge waves off southern Africa. *Continental Shelf Research*, 3, 343-357.

Slinger, J.H. & Taljaard, S. 1994. Preliminary investigation of seasonality in the Great Berg Estuary. Water SA 20: 279–288.

Slinger, J.H. and Taljaard, S. (1996) Water quality modelling of estuaries. Field data collection for calibrating the Mike 11 water quality module on the Great Berg Estuary. CSIR Data Report EMAS-D 96002. Stellenbosch.

Slinger, J.H, Taljaard, S. And Visser, E. (1996) Water quality modelling of estuaries. Field data collection for calibrating the Mike 11 water quality module on the Great Berg Estuary. CSIR Data Report EMAS-D 96004. Stellenbosch.

Taljaard, S., Slinger, J.H., Skibbe, E., Fricke, A.H., Kloppers, W.S. and Huizinga, P. (1992) Assessment of hydrodynamic and water quality aspects of the Berg River Estuary – 1989/990. CSIR Data Report EMAS-D 92006. Stellenbosch.